

General Disclaimer

One or more of the Following Statements may affect this Document

- This document has been reproduced from the best copy furnished by the organizational source. It is being released in the interest of making available as much information as possible.
- This document may contain data, which exceeds the sheet parameters. It was furnished in this condition by the organizational source and is the best copy available.
- This document may contain tone-on-tone or color graphs, charts and/or pictures, which have been reproduced in black and white.
- This document is paginated as submitted by the original source.
- Portions of this document are not fully legible due to the historical nature of some of the material. However, it is the best reproduction available from the original submission.

NCC2-149
51 pages

JOINT INSTITUTE FOR AERONAUTICS AND ACOUSTICS

National Aeronautics and
Space Administration
Ames Research Center

JIAA-TR 58



Stanford University

FLOW PAST A FLAT PLATE WITH A VORTEX/SINK COMBINATION

(NASA-CR-1769C8) FLOW PAST A FLAT PLATE
WITH A VORTEX/SINK COMBINATION (Stanford
Univ.) 51 p CSCI 20D

N86-29159

Unclas
G3/34 43360

Nikos J. Mourtos

STANFORD UNIVERSITY
Department of Aeronautics and Astronautics
Stanford, California 94305

SEPTEMBER 1984



JIAA TR - 58

**FLOW PAST A FLAT PLATE
WITH A VORTEX/SINK COMBINATION**

Nikos J. Mourtos

The work here presented has been supported by NASA Grant NCC 2-149.

SEPTEMBER 1984

ABSTRACT

An attempt has been made to model the so called "Leading Edge Vortex" which forms over the leading edge of delta wings at high angles of attack.

A simplified model has been considered, namely that of a two-dimensional, inviscid, incompressible steady flow around a flat plate at an angle of attack with a stationary vortex detached on top, as well as a sink to simulate the strong spanwise flow.

The results appear to agree qualitatively with experiments. A comparison has also been made between the lift and the drag of this model and the corresponding results for two classical solutions:

- (i) that of totally attached flow over the plate with the Kutta condition satisfied at the trailing edge only,
- (ii) the Helmholtz solution of totally separated flow over the plate.

NOMENCLATURE

English letter symbols:

a	radius of the cylinder.
b	length of the span of the plate.
c	chord length of the plate.
C_D	drag coefficient.
C_L	lift coefficient.
C_M	pitching moment coefficient.
C_P	pressure coefficient.
d	distance between the streamlines leading to the two stagnation points on the plate.
D	drag force.
F	total force on the plate.
k	total vortex strength.
k_0	bound vortex strength.
k_1	leading edge vortex strength.
K	non-dimensional total vortex strength.
K_0	non-dimensional bound vortex strength.
K_1	non-dimensional leading edge vortex strength.
L	lift force.
\dot{m}	mass flow rate.
m_1	sink strength.
M_1	non-dimensional sink strength.
n	non-dimensional parameter showing position along the plate.
r, θ	polar coordinates in the z -plane.
R_1	non-dimensional distance from the center of the cylinder to equilibrium point.
S	wing area.
u, v	velocity components.
V_∞	free stream velocity.
w	complex potential.
x, y	cartesian coordinates in the z -plane.
z	complex variable in the original circle plane.
\bar{z}	complex conjugate of z .
z'	complex variable in the rotated circle plane.

Greek letter symbols:

α	angle of attack.
Γ	total circulation.
Γ_0	circulation due to the bound vortex.
ζ	complex variable in the final plate plane.
ζ'	complex variable in the Joukowski plane.
ξ, η	coordinates in the ζ -plane.
ξ', η'	coordinates in the ζ' -plane.
Λ_0	doublet strength.
ρ	air density.

Subscripts:

c	in the plane of the cylinder.
p	in the plane of the plate.
r	radial component.
sc	on the surface of the cylinder.
sp	on the surface of the plate.
TE	at the trailing edge.
z	in the z -plane.
θ	tangential component.
ζ	in the ζ -plane.
0	refers to the origin (center of the cylinder).
1	refers to the equilibrium point.

TABLE OF CONTENTS

Abstract	i
Nomenclature	ii
Table of Contents	iv
List of Figures	vi
1. Introduction	1
2. Analysis of Flowfield	2
2.1 The Complex Potential	2
2.2 The Velocity Field	3
2.2.1 Radial Components	3
2.2.2 Tangential Components	3
2.3 Conformal Transformation Used to Analyze Flowfield	3
3. Conditions	5
3.1 Kutta Condition at Trailing Edge	5
3.2 Kutta Condition at Leading Edge	5
3.3 Vortex/Sink Velocity Condition	6
3.4 Non-Dimensional Parameters	8
3.5 Additional Condition	9

4. Results	11
4.1 Position of Equilibrium Point	11
4.2 Vortex and Sink Strengths	11
4.3 Pressure Distribution on the Plate	11
4.4 Lift, Drag, and Pitching Moment	13
5. Conclusions	15
References	16
Figures	17
Appendix 1	36
Appendix 2	37

LIST OF FIGURES

<i>Figure 1.</i>	Schematic of the flow over a slender sharp-edged wing.	18
<i>Figure 2.</i>	Steps in mapping sequence from original circle plane to final flat airfoil plane.	19
<i>Figure 3.</i>	Velocity components in cartesian and polar coordinate systems.	20
<i>Figure 4.</i>	Force diagram on the flat plate.	21
<i>Figure 5.</i>	Streamline pattern around the flat plate at an angle of attack with a detached vortex and a sink.	21
<i>Figure 6.</i>	Position of the equilibrium point (along the plate).	22
<i>Figure 7.</i>	Position of the equilibrium point (perpendicular to the plate).	23
<i>Figure 8.</i>	Leading edge and bound vortex strength versus angle of attack.	24
<i>Figure 9.</i>	Sink strength versus angle of attack.	25
<i>Figure 10.</i>	Total vortex strength versus angle of attack.	26
<i>Figure 11.</i>	Pressure distribution along the plate.	27
<i>Figure 12.</i>	Schematic of the flow over a flat plate at an angle of attack, according to three different models.	31
<i>Figure 13.</i>	Lift characteristics.	32

<i>Figure 14.</i>	Drag characteristics.	33
<i>Figure 15.</i>	Lift to drag ratio versus angle of attack.	34
<i>Figure 16.</i>	Pitching moment characteristics.	35

1. INTRODUCTION

So far there are two well-known models for the flow over a flat plate at an angle of attack. That of totally attached flow with the Kutta condition satisfied at the trailing edge only, and that of totally separated flow (Helmholtz solution).

The present model, considering partially separated flow lies somewhere between the two and despite the fact that it too is two-dimensional, gives some very useful representation of the three-dimensional flow over delta wings. On such wings the leading edge is usually sharp, causing thus flow separations even at moderate angles of attack. These flow separations take the form of two free vortex layers joined to the leading edge of the wing and rolling up to form spiral shaped vortices above the upper surface of the wing (Figure 1a).

These vortices induce additional velocities at the upper surface of the wing. The corresponding pressure distribution shows distinctly marked minima beneath the vortex axes (Figure 1b). Accordingly, an additional lift force occurs which depends nonlinearly on the angle of attack (Figure 1c).

In the theoretical study made here, a simplified model has been considered, namely that of a two-dimensional, inviscid, incompressible steady flow over a flat plate at an angle of attack, with a stationary vortex detached on top as well as a sink to simulate the strong spanwise flow caused by the pressure gradient due to sweep in the three-dimensional case.

2. ANALYSIS OF THE FLOW FIELD

In the original circle plane (also called z -plane) the flow field consists of the following components:

- (i) Uniform wind V_∞ coming from the negative x -axis.
- (ii) A doublet Λ_0 at the origin to simulate a circular cylinder $|z| = a$.
- (iii) A bound vortex k_0 at the origin to account for the circulation Γ_0 around the plate. Note that although the flow is aligned with the x -axis the plate is at an angle of attack, requiring thus circulation Γ_0 for the Kutta condition to be satisfied (see Figure 2a).
- (iv) A steady vortex k_1 of finite radius placed at $z_1(r_1, \theta_1)$ to simulate the leading edge vortex.
- (v) A steady vortex $-k_1$ at the inverse square point of z_1 induced by the circle theorem (see Appendix A1.1).
- (vi) A steady vortex k_1 at the origin also induced by the circle theorem (see Appendix A1.1).
- (vii) A sink m_1 ($m_1 < 0$) placed at $z_1(r_1, \theta_1)$ to simulate the spanwise flow along the center of the vortex.
- (viii) A sink m_1 at the inverse square point of z_1 , induced by the circle theorem (see Appendix A1.2).
- (ix) A source $-m_1$ at the origin also induced by the circle theorem (see Appendix A1.2).

2.1 The Complex Potential

For the components described above (regrouping them together), the complex potential is given below:

$$w = V_\infty \left(z + \frac{a^2}{z} \right) + (-m_1 + ik) \ln z + (m_1 + ik_1) \ln(z - z_1) + (m_1 - ik_1) \ln \left(z - \frac{a^2}{\bar{z}_1} \right) \quad (1)$$

where

$$k = k_0 + k_1 \quad (2)$$

2.2 The velocity Field

Differentiation of the complex potential gives the velocity field:

$$\frac{dw}{dz} = (u_r - iu_\theta) e^{-i\theta} \quad (3)$$

which applied to equation (1) gives:

2.2.1 Radial Components

$$u_r = V_\infty \left(1 - \frac{a^2}{r^2} \right) \cos \theta - \frac{m_1}{r} + \frac{m_1[r - r_1 \cos(\theta - \theta_1)] + k_1 r_1 \sin(\theta - \theta_1)}{r^2 + r_1^2 - 2rr_1 \cos(\theta - \theta_1)} + \frac{m_1 r_1 [rr_1 - a^2 \cos(\theta - \theta_1)] - k_1 r_1 a^2 \sin(\theta - \theta_1)}{r^2 r_1^2 + a^4 - 2rr_1 a^2 \cos(\theta - \theta_1)} \quad (4)$$

2.2.2 Tangential Components

$$u_\theta = -V_\infty \left(1 + \frac{a^2}{r^2} \right) \sin \theta - \frac{k}{r} + \frac{m_1 r_1 \sin(\theta - \theta_1) - k_1 [r - r_1 \cos(\theta - \theta_1)]}{r^2 + r_1^2 - 2rr_1 \cos(\theta - \theta_1)} + \frac{m_1 r_1 a^2 \sin(\theta - \theta_1) + k_1 r_1 [rr_1 - a^2 \cos(\theta - \theta_1)]}{r^2 r_1^2 + a^4 - 2rr_1 a^2 \cos(\theta - \theta_1)} \quad (5)$$

2.3 Conformal Transformation Used to Analyze the Flow Field

A solution for the flow field is provided by a mapping sequence that transforms the potential flow about a circle into a flow about a flat plate at an angle of attack with a detached vortex/sink combination. The steps are the following (see also Figure 2):

- original circle plane (z -plane),
- rotated circle plane (z' -plane), $z' = ze^{i\alpha}$,
- Joukowski plane (ζ' -plane), $\zeta' = z' + \frac{a^2}{z'}$,
- final plate plane (ζ -plane), $\zeta = \zeta' e^{-i\alpha}$.

The first step is a simple rotation in order to make the flat plate depicted inside the circle aligned with the x -axis. The second step is the Joukowski transformation which transforms the circle into a flat plate. The third step is another rotation which gives the plate an angle of attack with respect to the horizontal free stream velocity.

Combining the three steps we have that

$$\zeta = z + \frac{a^2}{z} e^{-2i\alpha} \quad (6)$$

or

$$z = \frac{\zeta}{2} \pm \sqrt{\left(\frac{\zeta}{2}\right)^2 - (ae^{-i\alpha})^2} \quad (7)$$

and if we set

$$\zeta = \xi + i\eta \quad (8)$$

we get

$$\xi = r \cos \theta + \frac{a^2}{r} \cos(\theta + 2\alpha) \quad (9)$$

$$\eta = r \sin \theta - \frac{a^2}{r} \sin(\theta + 2\alpha) \quad (10)$$

On the surface of the cylinder (corresponding to the surface of the plate) $r = a$ so

$$\xi_{sp} = a [\cos \theta + \cos(\theta + 2\alpha)] \quad (11)$$

$$\eta_{sp} = a [\sin \theta - \sin(\theta + 2\alpha)] \quad (12)$$

now

$$\frac{dw}{d\zeta} = \frac{dw}{dz} \cdot \frac{dz}{d\zeta} \quad (13)$$

and

$$\begin{aligned} \frac{dz}{d\zeta} &= \frac{1}{d\zeta/dz} \\ &= \frac{z^2 e^{2i\alpha}}{z^2 e^{2i\alpha} - a^2} \\ &= \frac{r^2 e^{i(2\alpha+2\theta)}}{r^2 e^{i(2\alpha+2\theta)} - a^2} \end{aligned}$$

Considering the surface again ($r = a$), expanding the right-hand side into sines and cosines and using equation (3) we get finally

$$[u_{r,sp}]_{\zeta} = \frac{\sin(4\theta + 4\alpha) - 2 \sin(2\theta + 2\alpha) - 2 \cos(2\theta + 2\alpha)}{2 + 2 \cos(4\theta + 4\alpha) - 4 \cos(2\theta + 2\alpha)} \cdot [u_{\theta,sc}]_z \quad (14)$$

$$[u_{\theta,sp}]_{\zeta} = -\frac{1}{2 \cos(2\theta + 2\alpha)} [u_{\theta,sc}]_z \quad (15)$$

3. CONDITIONS

Boundary conditions in the final plate plane require that:

(i) the flow depart smoothly from the trailing edge;

(ii) the flow depart smoothly from the leading edge, i.e., the Kutta condition must be satisfied at both edges of the plate.

Also, the vortex/sink combination must be located at an equilibrium point in the flow field, that is, a point where the velocity induced by all other components is zero.

3.1 Kutta Condition at the Trailing Edge

From equations (14) and (15) with $\theta = -\alpha$ we find the velocity components at the trailing edge of the plate:

$$[u_{r,sp}]_s^{TE} = -\frac{1}{0} [u_{\theta,sc}]_x^{\theta=-\alpha} \quad (16)$$

$$[u_{r,sp}]_s^{TE} = -\frac{1}{2} [u_{\theta,sc}]_x^{\theta=-\alpha} \quad (17)$$

For the Kutta condition to be satisfied there (i.e., u_r finite and $u_\theta = 0$) we must have

$$[u_{\theta,sc}]_x^{\theta=-\alpha} = 0 \quad (18)$$

or, from equation (5) with $r = a$ and $\theta = -\alpha$

$$(2V_\infty a \sin \alpha - k) [r_1^2 + a^2 - 2r_1 a \cos(\theta_1 + \alpha)] - 2m_1 r_1 a \sin(\theta_1 + \alpha) + k_1 (r_1^2 - a^2) = 0 \quad (19)$$

3.2 Kutta Condition at the Leading Edge

Similarly, for the leading edge we must have

$$[u_{\theta,sc}]_x^{\theta=\pi-\alpha} = 0 \quad (20)$$

and again from equation (5) with $r = a$ and $\theta = \pi - \alpha$

$$(2V_\infty a \sin \alpha + k) [r_1^2 + a^2 + 2r_1 a \cos(\theta_1 + \alpha)] - 2m_1 r_1 a \sin(\theta_1 + \alpha) - k_1 (r_1^2 - a^2) = 0 \quad (21)$$

3.3 Vortex/Sink Velocity Condition

Equation (3) cannot be used to find the conditions which make the velocity vanish at the location of the sink and vortex because the velocity given by equation (3) is singular there. Therefore, the usual limiting process has to be used to find the velocity components at the center of the vortex/sink combination. The strengths of the singularities can then be adjusted so that they are stationary in the presence of the plate. Following the analysis of reference 3 the complex velocity function in the final plate plane at the equilibrium point is found to be

$$[u_p - iv_p]_{z_1} = \left[(u_c - iv_c) \frac{dz}{d\zeta} \right]_{z_1} - \frac{1}{2} (m_1 + ik_1) \frac{[d^2z/d\zeta^2]_{z_1}}{[dz/d\zeta]_{z_1}} = 0 \quad (22)$$

The derivative $\frac{dz}{d\zeta}$ has been found in Section 2.3:

$$\frac{dz}{d\zeta} = \frac{(ze^{i\alpha})^2}{(ze^{i\alpha})^2 - a^2}$$

while

$$\frac{d^2z}{d\zeta^2} = \frac{d}{d\zeta} \left(\frac{dz}{d\zeta} \right) = \frac{d}{d\zeta} \left[\frac{z^2 e^{2i\alpha}}{z^2 e^{2i\alpha} - a^2} \right]$$

and substituting z from equation (7), taking the derivative and substituting back ζ from equation (6) we get

$$\frac{d^2z}{d\zeta^2} = \frac{a^2 e^{2i\alpha} [4z^4 + 3(z^2 + a^2 e^{-2i\alpha})^2]}{2z(a^2 e^{-2i\alpha} - z^2)(z^2 e^{2i\alpha} - a^2)^2}$$

Also, from Figure 3 we have the following transformations:

$$u_r = u_c \cos \theta + v_c \sin \theta$$

$$u_\theta = v_c \cos \theta - u_c \sin \theta$$

or

$$u_c = u_r \cos \theta - u_\theta \sin \theta$$

$$v_c = u_r \sin \theta + u_\theta \cos \theta$$

Substituting all these into equation (22) we get

$$\begin{aligned} & [(u_{r1} \cos \theta_1 - u_{\theta 1} \sin \theta_1) - i(u_{r1} \sin \theta_1 + u_{\theta 1} \cos \theta_1)] z_1^2 e^{2i\alpha} \\ & - (m_1 + ik_1) \frac{a^2 [4z_1^4 + 3(z_1^2 + a^2 e^{-2i\alpha})^2]}{2z_1(z_1^2 - a^2 e^{-2i\alpha})^2} = 0 \end{aligned} \quad (23)$$

where

$$z_1 = r_1 e^{i\theta_1} = r_1 (\cos \theta_1 + i \sin \theta_1) \quad (24)$$

Splitting into real and imaginary parts and substituting for u_{r_1} and u_{θ_1} their equivalent expressions from equations (4) and (5) with $r = r_1$ and $\theta = \theta_1$ we get

$$\begin{aligned} & 2V_\infty r_1^5 (r_1^2 - a^2)^2 \cos \theta_1 \cos(6\theta_1 + 2\alpha) - 4V_\infty r_1^3 a^2 (r_1^2 - a^2)^2 \cos \theta_1 \cos 4\theta_1 \\ & + 2V_\infty r_1 a^4 (r_1^2 - a^2)^2 \cos \theta_1 \cos(2\theta_1 - 2\alpha) - 2V_\infty r_1^5 (r_1^4 - a^4) \sin \theta_1 \sin(6\theta_1 + 2\alpha) \\ & + 4V_\infty r_1^3 a^2 (r_1^4 - a^4) \sin \theta_1 \sin 4\theta_1 - 2V_\infty r_1 a^4 (r_1^4 - a^4) \sin \theta_1 \sin(2\theta_1 - 2\alpha) \\ & - 2k_0 r_1^6 (r_1^2 - a^2) \sin(6\theta_1 + 2\alpha) + 4k_0 r_1^4 a^2 (r_1^2 - a^2) \sin 4\theta_1 \\ & - 2k_0 r_1^2 a^4 (r_1^2 - a^2) \sin(2\theta_1 - 2\alpha) + 2k_1 r_1^6 a^2 \sin(6\theta_1 + 2\alpha) \\ & + k_1 r_1^4 a^2 (7r_1^2 - 11a^2) \sin 4\theta_1 + 7k_1 r_1^4 a^2 (r_1^2 - a^2) \cos 4\theta_1 \\ & + 2k_1 r_1^2 a^4 (3r_1^2 - 2a^2) \sin(2\theta_1 - 2\alpha) + 6k_1 r_1^2 a^4 (r_1^2 - a^2) \cos(2\theta_1 - 2\alpha) \\ & + 3(k_1 - m_1)(r_1^2 - a^2)(\cos 4\alpha - \sin 4\alpha) a^6 + 2m_1 r_1^6 a^2 \cos(6\theta_1 + 2\alpha) \\ & - m_1 r_1^4 a^2 (7r_1^2 - 3a^2) \cos 4\theta_1 - 7m_1 r_1^4 a^2 (r_1^2 - a^2) \sin 4\theta_1 \\ & - 2m_1 r_1^2 a^4 (3r_1^2 - 4a^2) \cos(2\theta_1 - 2\alpha) - 6m_1 r_1^2 a^4 (r_1^2 - a^2) \sin(2\theta_1 - 2\alpha) = 0 \quad (25) \end{aligned}$$

and

$$\begin{aligned} & 2V_\infty r_1^5 (r_1^2 - a^2)^2 \cos \theta_1 \sin(6\theta_1 + 2\alpha) - 4V_\infty r_1^3 a^2 (r_1^2 - a^2)^2 \cos \theta_1 \sin 4\theta_1 \\ & + 2V_\infty r_1 a^4 (r_1^2 - a^2)^2 \cos \theta_1 \sin(2\theta_1 - 2\alpha) + 2V_\infty r_1^5 (r_1^4 - a^4) \sin \theta_1 \cos(6\theta_1 + 2\alpha) \\ & - 4V_\infty r_1^3 a^2 (r_1^4 - a^4) \sin \theta_1 \cos 4\theta_1 + 2V_\infty r_1 a^4 (r_1^4 - a^4) \sin \theta_1 \cos(2\theta_1 - 2\alpha) \\ & + 2k_0 r_1^6 (r_1^2 - a^2) \cos(6\theta_1 + 2\alpha) - 4k_0 r_1^4 a^2 (r_1^2 - a^2) \cos 4\theta_1 \\ & + 2k_0 r_1^2 a^4 (r_1^2 - a^2) \cos(2\theta_1 - 2\alpha) - 2k_1 r_1^6 a^2 \cos(6\theta_1 + 2\alpha) \\ & - k_1 r_1^4 a^2 (7r_1^2 - 11a^2) \cos 4\theta_1 - 7k_1 r_1^4 a^2 (r_1^2 - a^2) \sin 4\theta_1 \\ & - 2k_1 r_1^2 a^4 (3r_1^2 - 2a^2) \cos(2\theta_1 - 2\alpha) - 6k_1 r_1^2 a^4 (r_1^2 - a^2) \sin(2\theta_1 - 2\alpha) \\ & - 3(k_1 + m_1)(r_1^2 - a^2) a^6 (\cos 4\alpha - \sin 4\alpha) + 2m_1 r_1^6 a^2 \sin(6\theta_1 + 2\alpha) \\ & - m_1 r_1^4 a^2 (7r_1^2 - 3a^2) \sin 4\theta_1 - 7m_1 r_1^4 a^2 (r_1^2 - a^2) \cos 4\theta_1 \\ & - 2m_1 r_1^2 a^4 (3r_1^2 - 4a^2) \sin(2\theta_1 - 2\alpha) - 6m_1 r_1^2 a^4 (r_1^2 - a^2) \cos(2\theta_1 - 2\alpha) = 0 \quad (26) \end{aligned}$$

3.4 Non-Dimensional Parameters

At this point some non-dimensional parameters have to be introduced if the system of equations (19), (21), (25), and (26) is to be solved explicitly. These are the following:

$$K_0 = \frac{k_0}{aV_\infty} \quad (27)$$

$$K_1 = \frac{k_1}{aV_\infty} \quad (28)$$

$$K = \frac{k}{aV_\infty} \quad (29)$$

$$M_1 = \frac{m_1}{aV_\infty} \quad (30)$$

$$R_1 = \frac{r_1}{a} \quad (31)$$

Substitution into the original equations yields the following system of four equations in five unknowns K_0 , K_1 , M_1 , R_1 , and θ_1 :

$$(2 \sin \alpha - K)[R_1^2 + 1 - 2R_1 \cos(\theta_1 + \alpha)] - 2M_1 R_1 \sin(\theta_1 + \alpha) + K_1(R_1^2 - 1) = 0 \quad (32)$$

$$(2 \sin \alpha + K)[R_1^2 + 1 + 2R_1 \cos(\theta_1 + \alpha)] - 2M_1 R_1 \sin(\theta_1 + \alpha) - K_1(R_1^2 - 1) = 0 \quad (33)$$

$$\begin{aligned} & 2R_1^5(R_1^2 - 1)^2 \cos \theta_1 \cos(6\theta_1 + 2\alpha) - 4R_1^3(R_1^2 - 1)^2 \cos \theta_1 \cos 4\theta_1 \\ & + 2R_1(R_1^2 - 1)^2 \cos \theta_1 \cos(2\theta_1 - 2\alpha) - 2R_1^5(R_1^4 - 1) \sin \theta_1 \sin(6\theta_1 + 2\alpha) \\ & + 4R_1^3(R_1^4 - 1) \sin \theta_1 \sin 4\theta_1 - 2R_1(R_1^4 - 1) \sin \theta_1 \sin(2\theta_1 - 2\alpha) \\ & - 2K_0 R_1^6(R_1^2 - 1) \sin(6\theta_1 + 2\alpha) + 4K_0 R_1^4(R_1^2 - 1) \sin 4\theta_1 \\ & - 2K_0 R_1^2(R_1^2 - 1) \sin(2\theta_1 - 2\alpha) + 2K_1 R_1^6 \sin(6\theta_1 + 2\alpha) \\ & + K_1 R_1^4(7R_1^2 - 11) \sin 4\theta_1 + 7K_1 R_1^4(R_1^2 - 1) \cos 4\theta_1 \\ & + 2K_1 R_1^2(3R_1^2 - 2) \sin(2\theta_1 - 2\alpha) + 6K_1 R_1^2(R_1^2 - 1) \cos(2\theta_1 - 2\alpha) \\ & + 3(K_1 - M_1)(R_1^2 - 1)(\cos 4\alpha - \sin 4\alpha) + 2M_1 R_1^6 \cos(6\theta_1 + 2\alpha) \\ & - M_1 R_1^4(7R_1^2 - 3) \cos 4\theta_1 - 7M_1 R_1^4(R_1^2 - 1) \sin 4\theta_1 \\ & - 2M_1 R_1^2(3R_1^2 - 4) \cos(2\theta_1 - 2\alpha) - 6M_1 R_1^2(R_1^2 - 1) \sin(2\theta_1 - 2\alpha) = 0 \quad (34) \end{aligned}$$

$$\begin{aligned} & 2R_1^5(R_1^2 - 1)^2 \cos \theta_1 \sin(6\theta_1 + 2\alpha) - 4R_1^3(R_1^2 - 1)^2 \cos \theta_1 \sin 4\theta_1 \\ & + 2R_1(R_1^2 - 1)^2 \cos \theta_1 \sin(2\theta_1 - 2\alpha) + 2R_1^5(R_1^4 - 1) \sin \theta_1 \cos(6\theta_1 + 2\alpha) \end{aligned}$$

$$\begin{aligned}
& -4R_1^3(R_1^4 - 1) \sin \theta_1 \cos 4\theta_1 + 2R_1(R_1^4 - 1) \sin \theta_1 \cos(2\theta_1 - 2\alpha) \\
& + 2K_0R_1^6(R_1^2 - 1) \cos(6\theta_1 + 2\alpha) - 4K_0R_1^4(R_1^2 - 1) \cos 4\theta_1 \\
& + 2K_0R_1^2(R_1^2 - 1) \cos(2\theta_1 - 2\alpha) - 2K_1R_1^6 \cos(6\theta_1 + 2\alpha) \\
& - K_1R_1^4(7R_1^2 - 11) \cos 4\theta_1 - 7K_1R_1^4(R_1^2 - 1) \sin 4\theta_1 \\
& - 2K_1R_1^2(3R_1^2 - 2) \cos(2\theta_1 - 2\alpha) - 6K_1R_1^2(R_1^2 - 1) \sin(2\theta_1 - 2\alpha) \\
& - 3(K_1 + M_1)(R_1^2 - 1)(\cos 4\alpha - \sin 4\alpha) + 2M_1R_1^6 \sin(6\theta_1 + 2\alpha) \\
& - M_1R_1^4(7R_1^2 - 3) \sin 4\theta_1 - 7M_1R_1^4(R_1^2 - 1) \cos 4\theta_1 \\
& - 2M_1R_1^2(3R_1^2 - 4) \sin(2\theta_1 - 2\alpha) - 6M_1R_1^2(R_1^2 - 1) \cos(2\theta_1 - 2\alpha) = 0 \quad (35)
\end{aligned}$$

3.5 Additional Condition

We see that the equations derived so far are not enough to give us a unique solution. Therefore we must seek additional information in the nature of the flow. As mentioned in the introduction the flow is assumed inviscid which implies that the total force on the plate must be perpendicular to it (see Figure 4). Therefore

$$\tan \alpha = \frac{D}{L} \quad (36)$$

Now we have to relate the drag and the lift with the unknowns K and M_1 .

From Figure 5 we see that the fluid between streamlines a and b disappears into the sink producing drag which can be calculated as follows: The rate of mass of fluid between the streamlines a and b (which is distance d apart) must be equal to the rate with which mass is disappearing in the sink, i.e.,

$$\dot{m} = -\rho V_\infty db = m_1 \rho b 2\pi. \quad (37)$$

Now the drag is given by the rate of loss of momentum of that fluid therefore

$$D = -\dot{m} V_\infty \quad (38)$$

combining equations (37) and (38) we get

$$m_1 = -\frac{D}{2\pi \rho b V_\infty} \quad (39)$$

and from equation (30) we get

$$M_1 = -\frac{D}{2\pi\rho b a V_\infty^2} \quad (40)$$

but

$$S = bc \quad (41)$$

and from the Joukowski transformation we know that

$$c = 4a \quad (42)$$

also,

$$C_D = \frac{D}{\frac{1}{2}\rho V_\infty^2 S} \quad (43)$$

The last four equations combine to give

$$C_D = -\pi M_1 \quad (44)$$

The lift can be found from the Kutta-Joukowski law

$$L = \rho V_\infty \Gamma \cdot b \quad (45)$$

and since

$$\Gamma = 2\pi k \quad (46)$$

and

$$C_L = \frac{L}{\frac{1}{2}\rho V_\infty^2 S} \quad (47)$$

we get

$$C_L = \pi K \quad (48)$$

after employing equation (29).

Now going back to equation (36) we see that

$$\tan \alpha = -\frac{M_1}{K} \quad (49)$$

thus we have a system of five equations (32)–(35) and (49), which can be solved for the five unknowns: R_1 , θ_1 , K_0 , K_1 , and M_1 . This is done numerically (see Appendix 2) and the results are shown in the next section.

4. RESULTS

4.1 Position of the Equilibrium Point

As it can be seen from Figure 6 the equilibrium point is always ahead of the leading edge of the plate and it goes farther as the angle of attack increases reaching a maximum distance of approximately 53 percent of the chord from the leading edge (measured along the chord line) at 45 degrees angle of attack.

At the same time (see Figure 7) after reaching a maximum distance above the chord line of approximately 16 percent of the chord (measured perpendicular to the chord line), it starts moving downwards crossing the chord line at $\alpha \simeq 35^\circ$ and getting farther under it at higher angles of attack.

4.2 Vortex and Sink Strengths

The bound vortex strength increases almost linearly with angle of attack while the leading edge vortex strength grows nonlinearly reaching a maximum at $\alpha = 45^\circ$ and dropping to zero at $\alpha \simeq 73^\circ$ where the lower stagnation point reaches the trailing edge and moves off the plate (Figure 8). Thus the total circulation is also nonlinear with angle of attack and has a maximum at $\alpha = 50^\circ$ (Figure 10). The sink strength on the other hand, starting with very small values increases almost linearly with angle of attack (Figure 9).

4.3 Pressure Distribution on the Plate

The pressure distribution has been calculated at the ζ' plane (the most convenient one since the plate is horizontal and lies along the ξ' -axis).

From the sequence of transformations shown in Figure 2 we have

$$\begin{aligned}\zeta' &= z' + \frac{a^2}{z'} \\ &= ze^{i\alpha} + \frac{a^2}{z} e^{-i\alpha} \\ &= re^{i\theta} e^{i\alpha} + \frac{a^2}{r} e^{-i\alpha} e^{-i\theta}\end{aligned}$$

or

$$\zeta' = r [\cos(\theta + \alpha) + i \sin(\theta + \alpha)] + \frac{a^2}{r} [\cos(\theta + \alpha) - i \sin(\theta + \alpha)].$$

and since

$$\zeta' = \xi' + i\eta' \quad (50)$$

we have

$$\xi' = \left(r + \frac{a^2}{r} \right) \cos(\theta + \alpha) \quad (51)$$

and

$$\eta' = \left(r - \frac{a^2}{r} \right) \sin(\theta + \alpha) \quad (52)$$

on the surface of the plate $r = a$ so

$$\xi'_{sp} = 2a \cos(\theta + \alpha) \quad (53)$$

$$\eta'_{sp} = 0 \quad (54)$$

To find the velocity field around the plate, a similar procedure as in Section 2.3 yields:

$$\begin{aligned} \frac{dw}{d\zeta'} &= \frac{dw}{dz} \cdot \frac{dz}{d\zeta'} \\ &= \frac{dw}{dz} \cdot \frac{z^2}{z^2 e^{i\alpha} - a^2 e^{-i\alpha}} \end{aligned}$$

or

$$e^{-i\theta} (u_{r_p} - iu_{\theta_p}) = e^{-i\theta} (u_{r_c} - iu_{\theta_c}) \cdot \frac{r^2 e^{i2\theta}}{r^2 e^{i(2\theta+\alpha)} - a^2 e^{-i\alpha}}$$

and on the surface ($r = a$) we get finally

$$u_{r_{sp}} = -\frac{1}{2} \cdot \frac{\cos \theta}{\sin(\theta + \alpha)} u_{\theta_{sc}} \quad (55)$$

$$u_{\theta_{sp}} = -\frac{1}{2} \cdot \frac{\sin \theta}{\sin(\theta + \alpha)} u_{\theta_{sc}} \quad (56)$$

from which

$$u_{sp} = \frac{1}{2} u_{\theta_{sc}} \csc(\theta + \alpha) \quad (57)$$

Now from equation (5) and using equations (27)-(31) we find that

$$\frac{u_{\theta_{sc}}}{V_{\infty}} = -2 \sin \theta - K + \frac{2M_1 R_1 \sin(\theta - \theta_1) + K_1 (R_1^2 - 1)}{1 + R_1^2 - 2R_1 \cos(\theta - \theta_1)} \quad (58)$$

Substituting equation (58) into (57) as well as the corresponding solution sets for each angle of attack we can find the pressure distribution from

$$C_{p,sp} = 1 - \frac{u_{sp}^2}{V_\infty^2} \quad (59)$$

$C_{p,sp}$ has been plotted for four angles of attack in Figure 11 where the horizontal axis measures the non-dimensional parameter

$$n = \cos(\theta + \alpha) = \frac{\xi'_{sp}}{2a}$$

which varies from -1 at the leading edge to $+1$ at the trailing edge.

It can be seen from the plottings that both stagnation points move towards the trailing edge as the angle of attack increases but the lower one moves faster, being at about 70 percent of the chord from the leading edge at $\alpha = 60^\circ$ while the upper one is only at the mid-chord point.

4.4 Lift, Drag, and Pitching Moment

At this point a comparison will be made between the results of:

- (i) the classical solution of totally attached flow over the plate with the Kutta condition satisfied at the trailing edge only and a singularity (infinite suction) at the leading edge (Figure 12a),
- (ii) this model with a detached vortex and a sink which make possible the satisfaction of the Kutta condition at both edges removing thus the leading edge singularity (Figure 12b),
- (iii) the Helmholtz solution of totally separated flow over the plate (Figure 12c).

The lift, drag and moment coefficients for the three models are given below:

$$C_{L1} = 2\pi \sin \alpha \quad C_{D1} = 0 \quad C_{M1} = \frac{\pi}{4} \sin 2\alpha \quad (60)$$

$$C_{L2} = \pi K \quad C_{D2} = -\pi M_1 \quad C_{M2} = \frac{\pi}{4} \sin 2\alpha \quad (61)$$

$$C_{L3} = \frac{\pi \sin 2\alpha}{4 + \pi \sin \alpha} \quad C_{D3} = \frac{2\pi \sin^2 \alpha}{4 + \pi \sin \alpha} \quad (62)$$

From Figure 13 it can be seen that our model with partially separated flow (as the leading edge vortex can be thought of), gives the highest lift coefficient at least up to $\alpha = 60^\circ$.

At higher angles it looks like the first model gives slightly higher lift coefficients, but this is misleading since at high angles of attack the flow separates at some point on the upper surface, resulting in significantly lower lift coefficients. Thus the first model breaks down at high angles of attack.

From Figure 14 it can be seen that our model gives much higher drag coefficients even than the third model in which the flow is totally separated on the upper surface of the plate. This should not be surprising however, because the drag in our model is associated with a large momentum loss of all the fluid that disappears into the sink (see Figure 5).

As a confirmation to the above comes Figure 15 which shows the same lift to drag ratio for the second and third models (since $L/D = \tan \alpha$ in both cases). In other words since the second model yields a much higher lift than the third one, it also gives a much higher drag which can be thought of as induced drag (lift related drag).

Finally, it is interesting to note that our model has the same moment coefficient and the same position of aerodynamic center (at the quarter chord point) as the first model. The proof is as follows: Since there is a uniform wind, the velocity at a great distance from the plate must tend simply to the wind velocity, and therefore if $|z|$ is sufficiently large we may write

$$\frac{dw}{dz} = V_\infty + \frac{A}{z} + \frac{B}{z^2} + \dots$$

or

$$w = V_\infty z + A \ln z + \frac{B}{z} + \dots$$

Now the force and the moment on the plate can be found from the theorem of Blasius and it turns out (after performing the integration) that the force depends only on A while the moment depends only on B . However, comparing the complex potential for the first two models we can see that B is the same regardless of the presence of the vortex/sink combination and therefore the moment ought to be the same for the two models. In equations (60) and (61) C_M is taken about the mid-point of the plate and is therefore positive. The same relations but with a minus sign on the right hand side are valid for C_M about the leading edge. Equations (60) and (61) are plotted in Figure 16.

5. CONCLUSIONS

- (i) The present inviscid, incompressible, two-dimensional model of a flat plate with a detached vortex close to its leading edge indicates that lift coefficients up to around 6 are achievable. Higher values should also be possible if thickness and camber are added, considering an airfoil instead of a flat plate (reference 3).
- (ii) In order to satisfy the Kutta condition at both the trailing edge and the leading edge, the presence of the sink is necessary (see equations (32) and (33)). This is in agreement with physical observations of the leading edge vortex which forms over delta wings at high angles of attack where the spanwise pressure gradient due to sweep angle evacuates the vortex core. It is also in agreement with the model presented in reference 3.
- (iii) For a given lift (C_L) there are two possible solutions for the location of the equilibrium point and the corresponding strengths of the vortex and sink. That of the lower angle of attack gives a weaker sink and therefore less drag, while that of the higher angle of attack gives a stronger sink and the associated higher drag. The vortex strengths do not differ much for the two solutions since they are closely related to the lift (which is the same for the two solutions). This result is also in agreement with reference 3.
- (iv) The upper limit found in the C_L versus α curve suggests that if a stronger vortex would exist at the equilibrium point, unrealistic supercirculation would occur resulting in the streamlines going entirely around the system.
- (v) A limitation of the present model appears at $\alpha \simeq 73^\circ$, above which the lower stagnation point moves off the plate making thus impossible the flow pattern depicted in Figure 5, on which this model is based.
- (vi) A comparison between Figures 8 and 1c shows very good agreement (at least qualitatively) between the results derived here and those found experimentally in reference 1.
- (vii) Finally, the presence of the vortex and the sink does not affect the position of the aerodynamic center which remains at the quarter chord point.

REFERENCES

1. Hummel, D. "On the Vortex Formation Over a Slender Wing at Large Angles of Incidence," *AGARD CP-247*, no. 15, 1978.
2. Milne-Thomson, L. M. *Theoretical Aerodynamics*. New York: Dover, 1958.
3. Rossow, V. J. "Lift Enhancement by an Externally Trapped Vortex," *J. Aircraft*, 15, no. 9 (1978), 618.
4. Milne-Thomson, L. M. *Theoretical Hydrodynamics*, London: MacMillan Press, 1968.
5. Rossow, V. J. "On the Inviscid Rolled-Up Structure of Lift-Generated Vortices," *J. Aircraft*, 10, no. 11 (1973), 647.
6. Hoeijmakers, H.W.M. and B. Bennekens, "A Computational Model for the Calculation of the Flow About Wings With Leading-Edge Vortices," *AGARD CP-247*, no. 25, 1978.
7. Bradley, R. G., C. W. Smith, and I. C. Bateley, "Vortex-Lift Prediction for Complex Wing Planforms," *J. Aircraft*, 10, no. 6 (1973), 379.
8. Peake, D. J. and M. Tobak, "Three-Dimensional Flows About Simple Components at Angle of Attack," *AGARD LS-121*, no. 2, 1982.
9. Skow, A. M. and G. E. Erickson, "Modern Fighter Aircraft Design for High Angle of Attack Maneuvering," *AGARD LS-121*, no. 4, 1982.
10. Lamar, J. E. and J. F. Campbell, "Recent Studies at NASA-Langley of Vortical Flows Interacting With Neighbouring Surfaces," *AGARD CP-342*, no. 10, 1983.

Figures

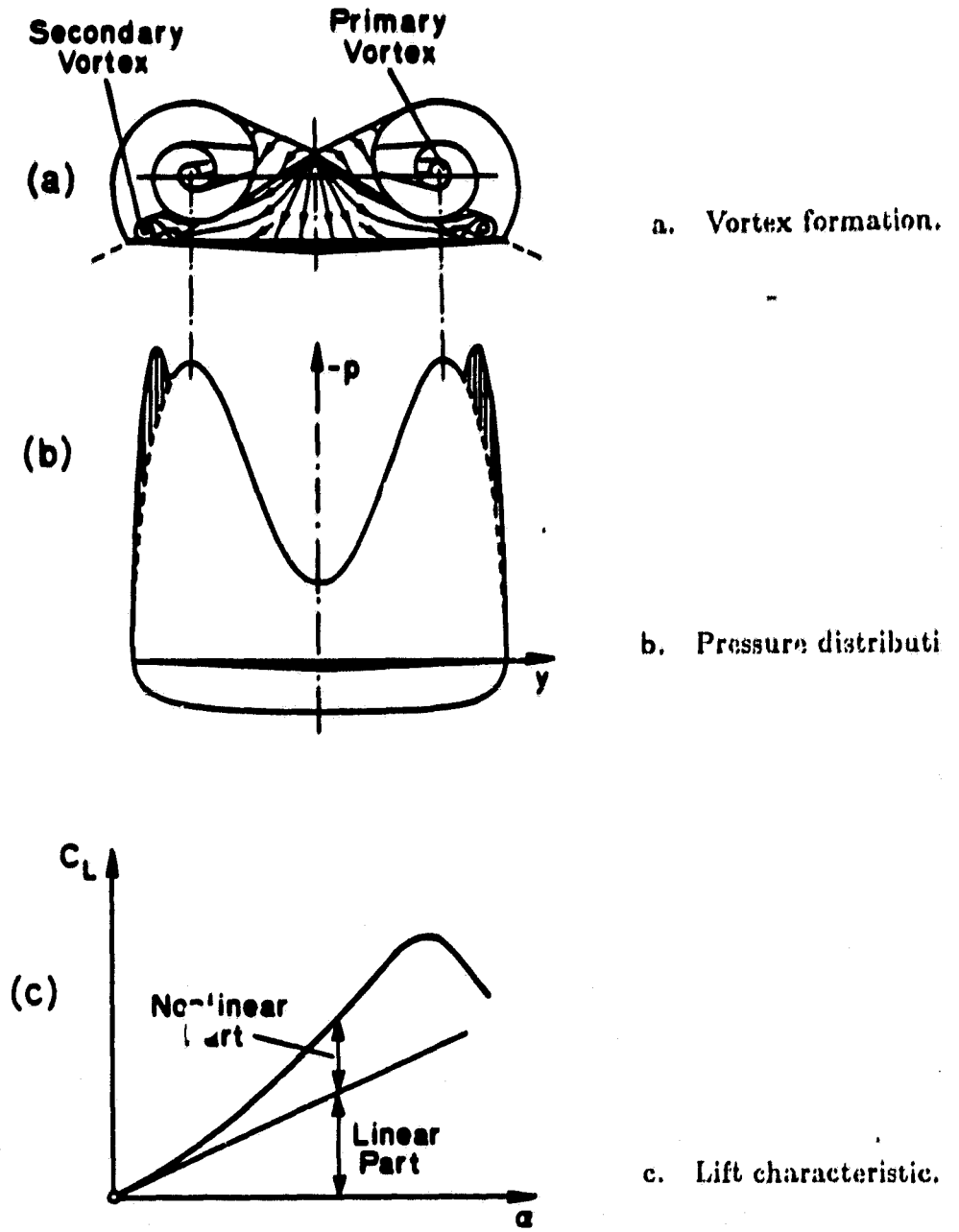
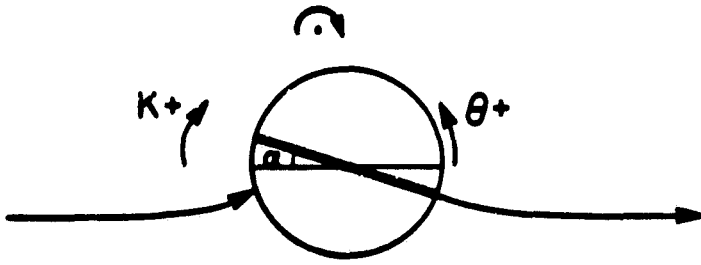
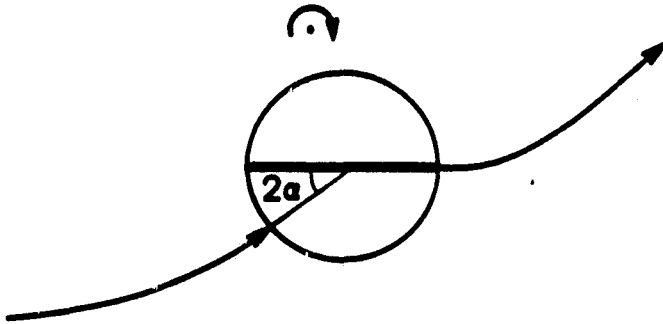


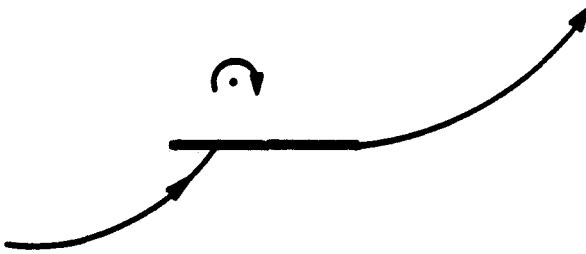
Figure 1. Schematic of the flow over a slender sharp-edged wing.



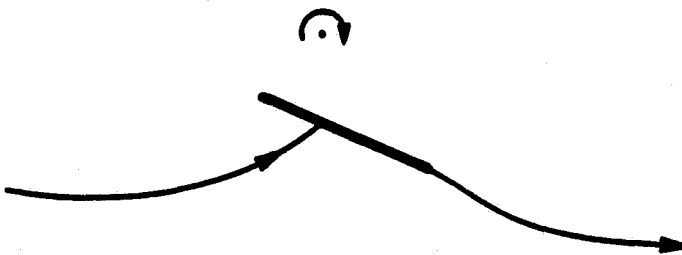
a. Original circle plane (z -plane).



b. Rotated circle plane (z' -plane).



c. Joukowski plane (ζ' -plane).



d. Final plate plane (ζ -plane).

Figure 2. Steps in mapping sequence from original circle plane to final flat airfoil plane.

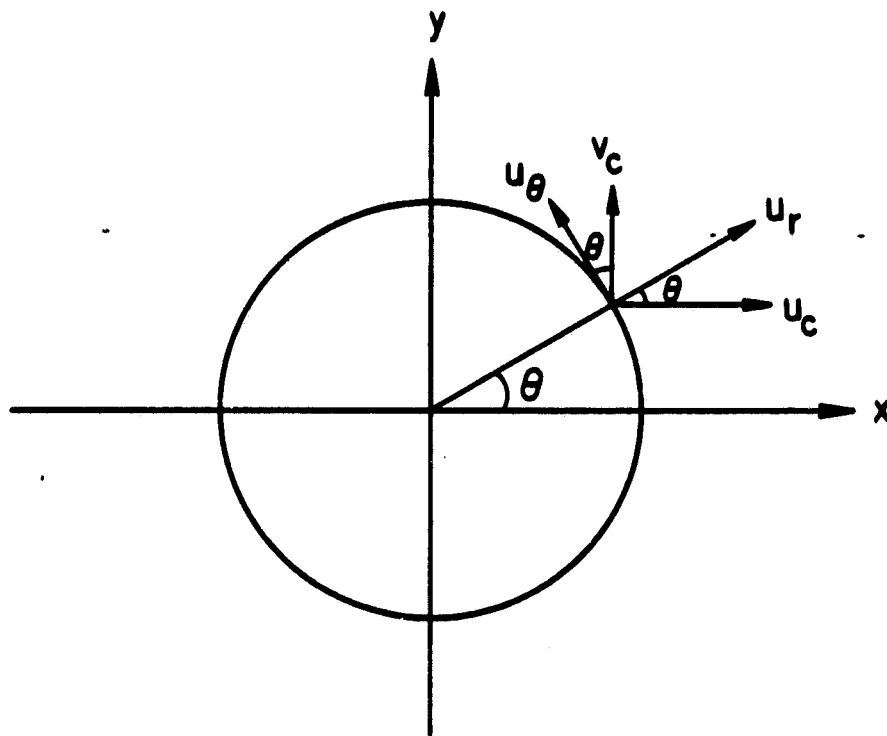


Figure 3. Velocity components in cartesian and polar coordinate systems.

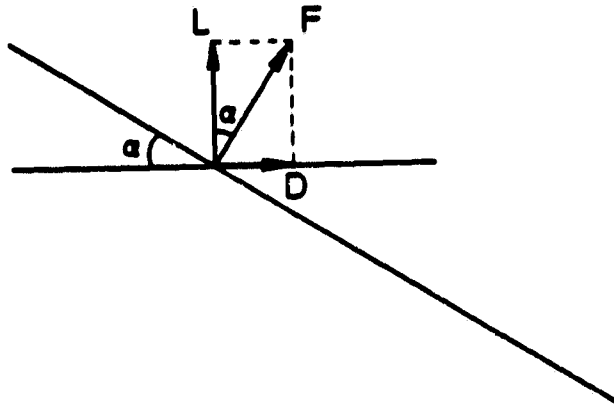


Figure 4. Force diagram on the flat plate.

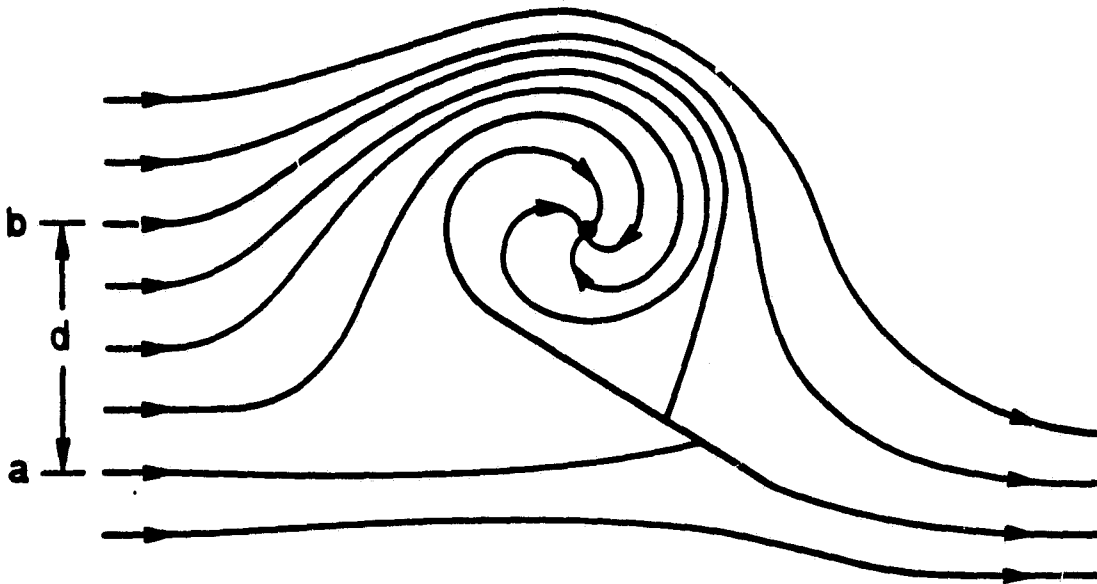


Figure 5. Streamline pattern around the flat plate at an angle of attack with a detached vortex and a sink.

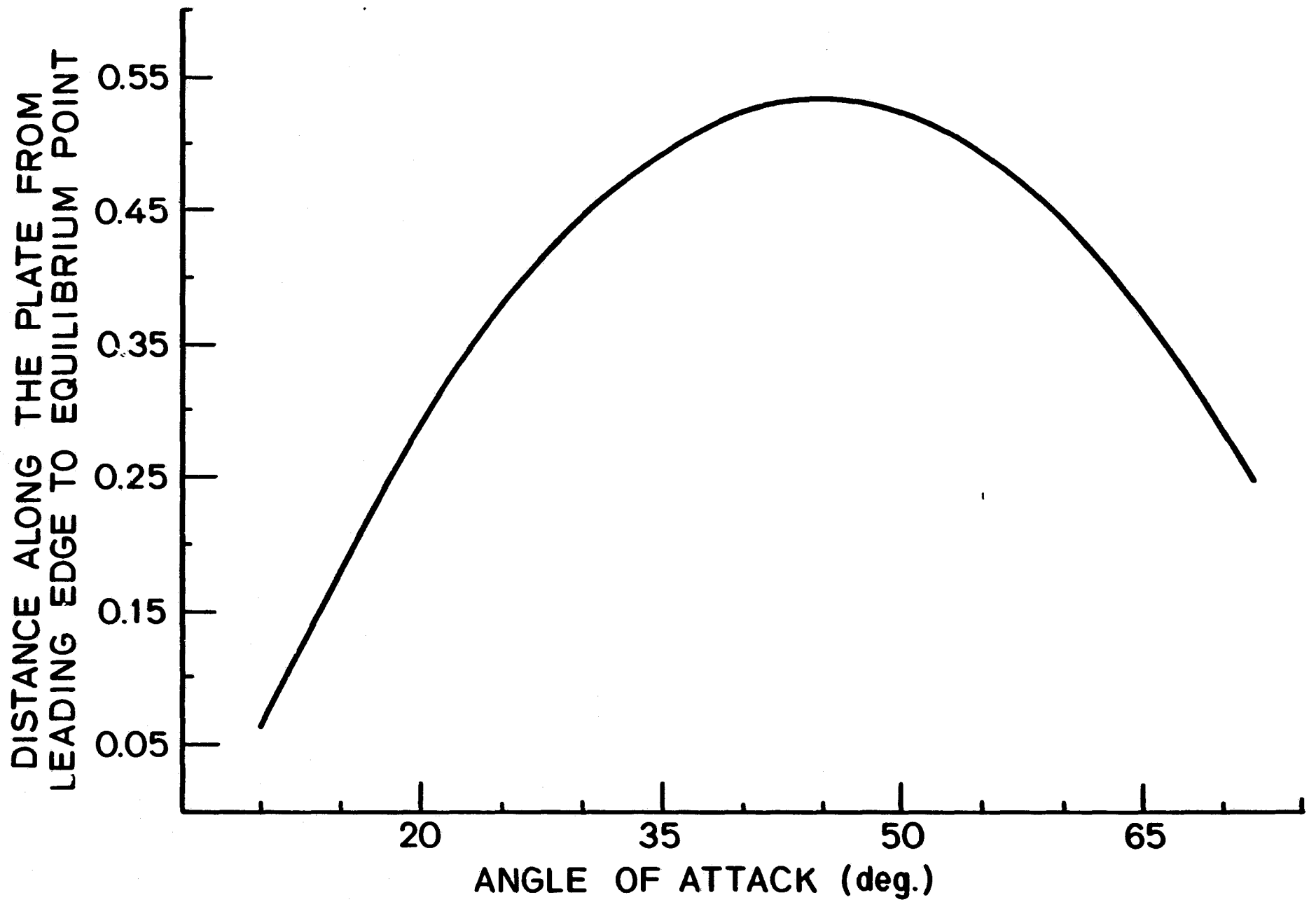


Figure 6. Position of the equilibrium point (along the plate).

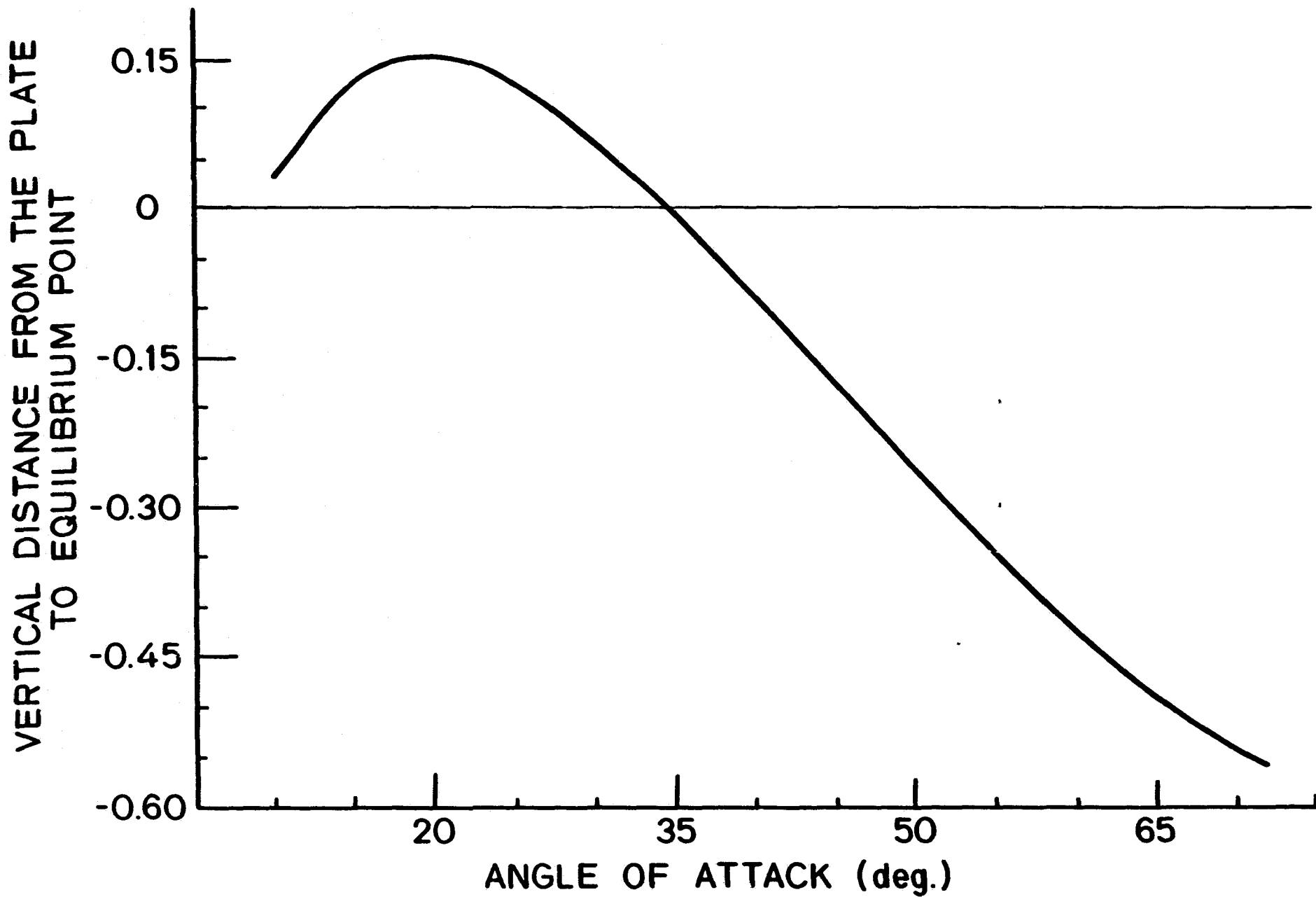


Figure 7. Position of the equilibrium point (perpendicular to the plate).

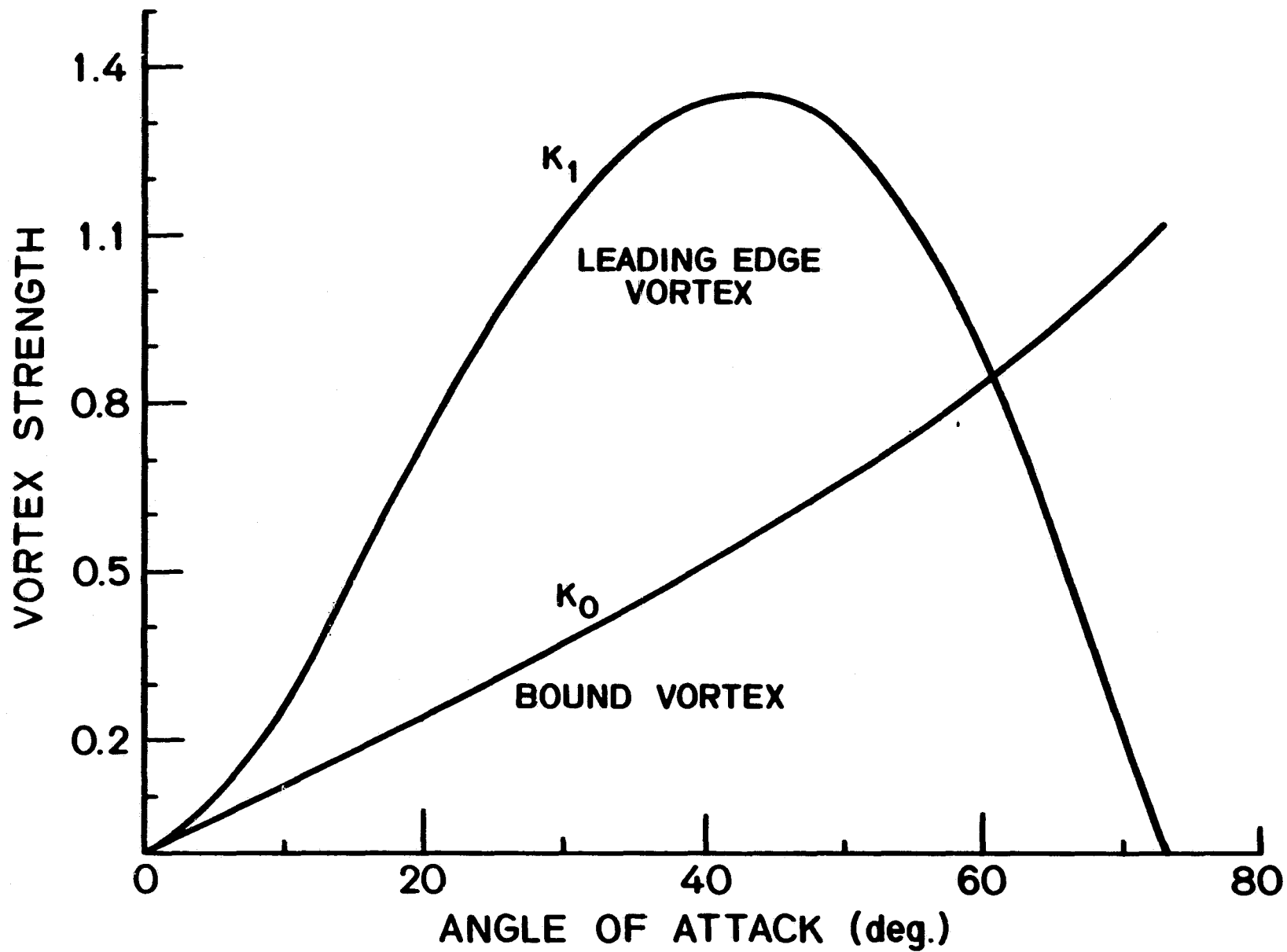


Figure 8. Leading edge and bound vortex strength versus angle of attack.

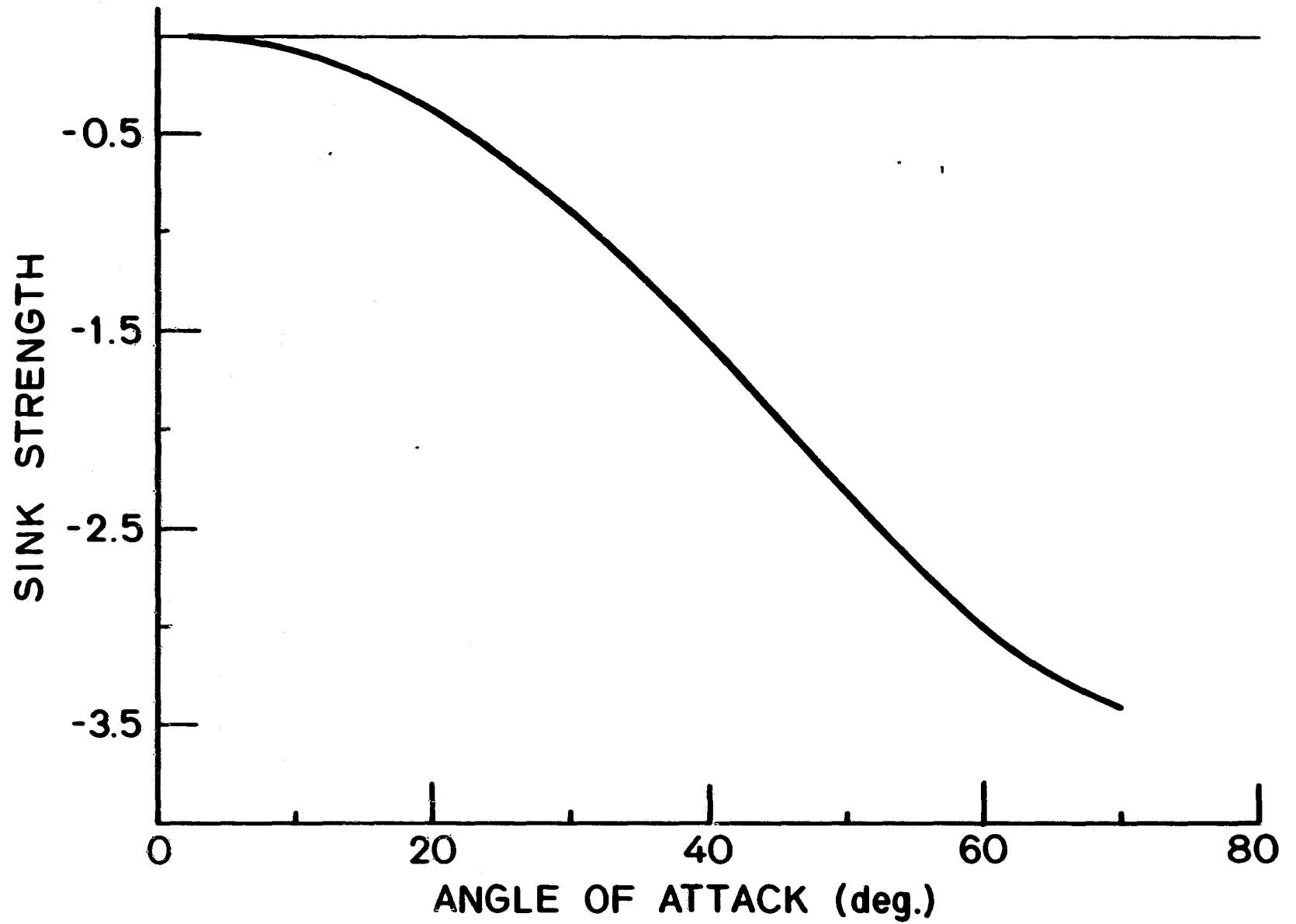


Figure 9. Sink strength versus angle of attack.

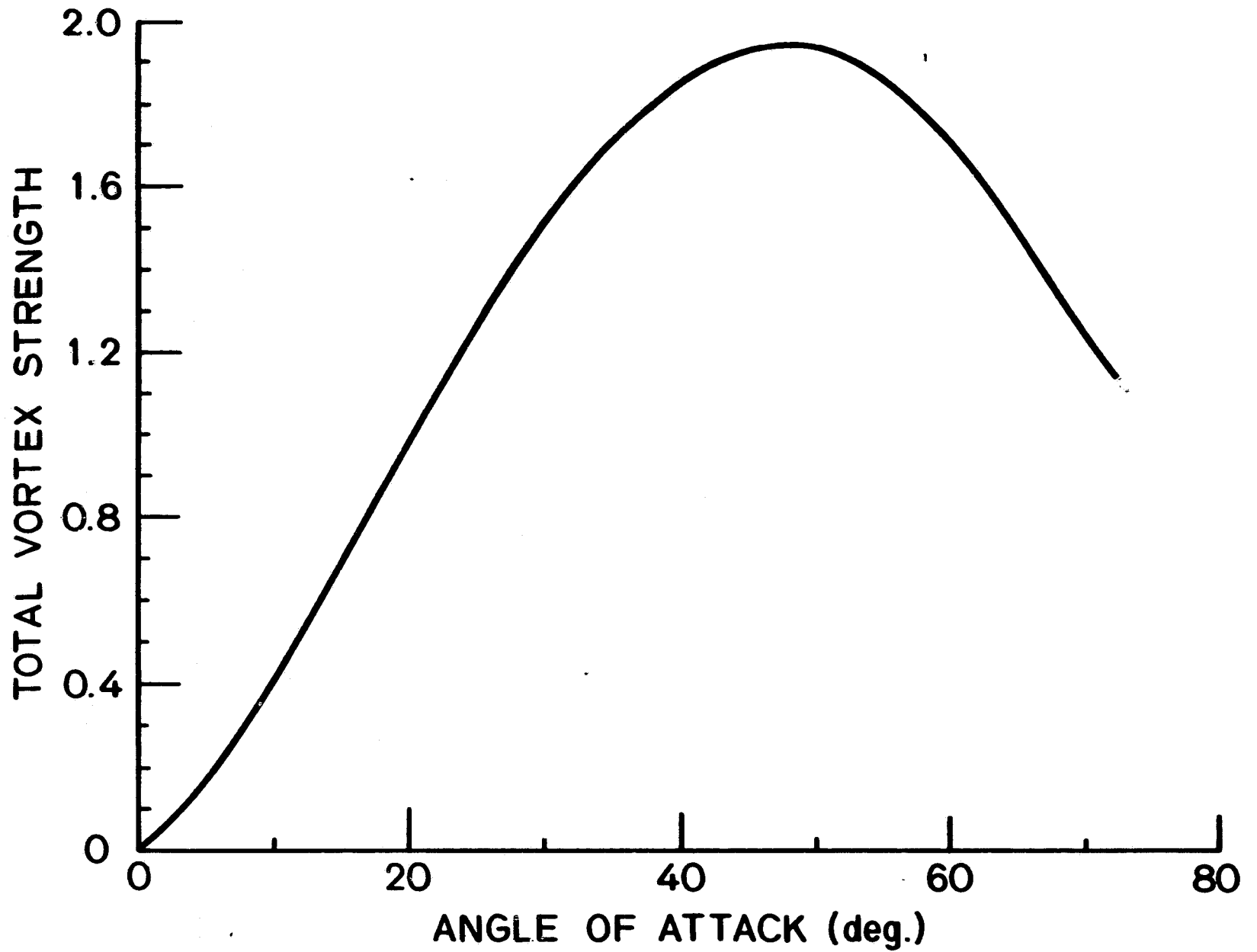


Figure 10. Total vortex strength versus angle of attack.

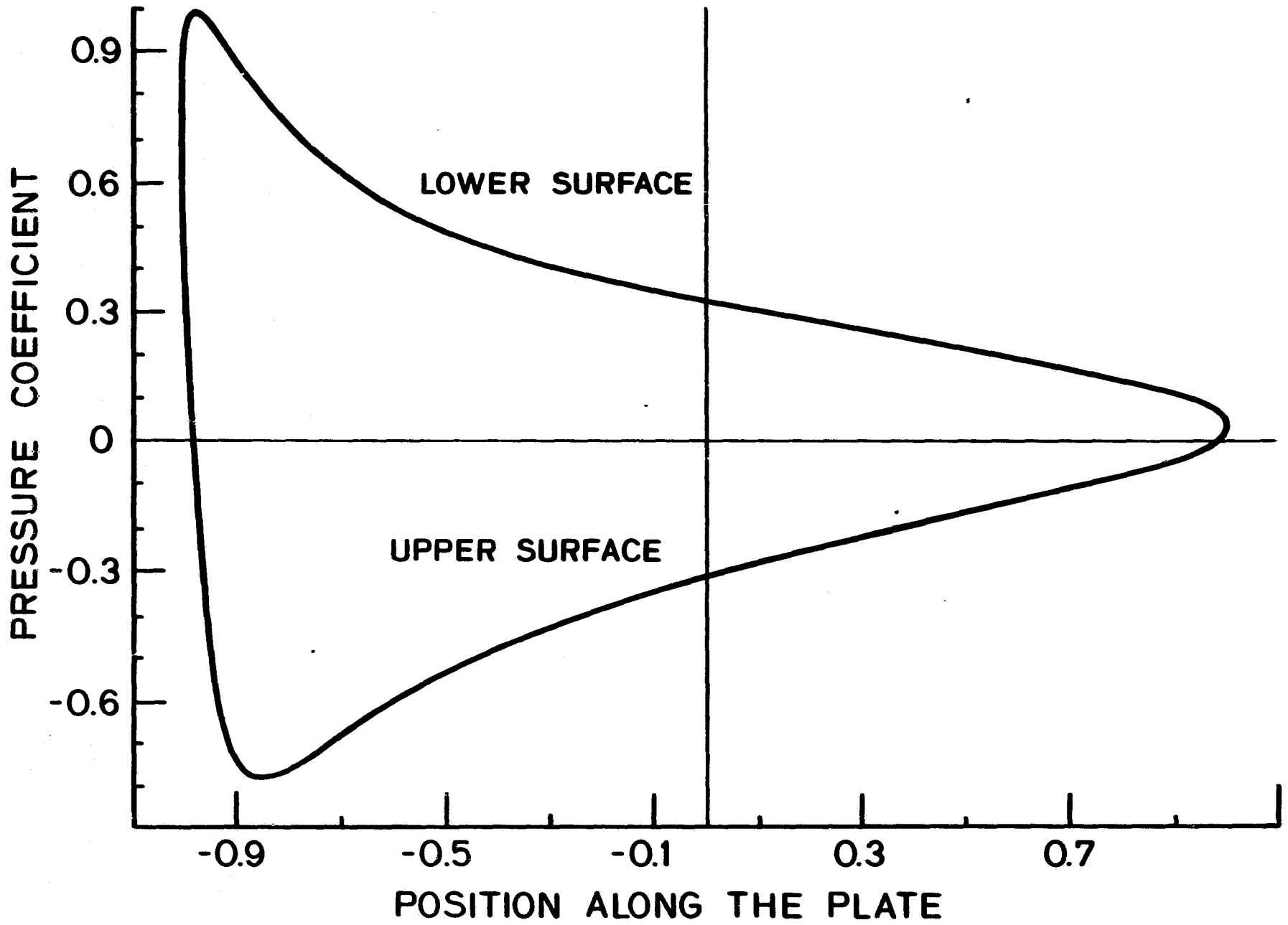


Figure 11a. Pressure distribution along the plate for $\alpha = 10$ deg.

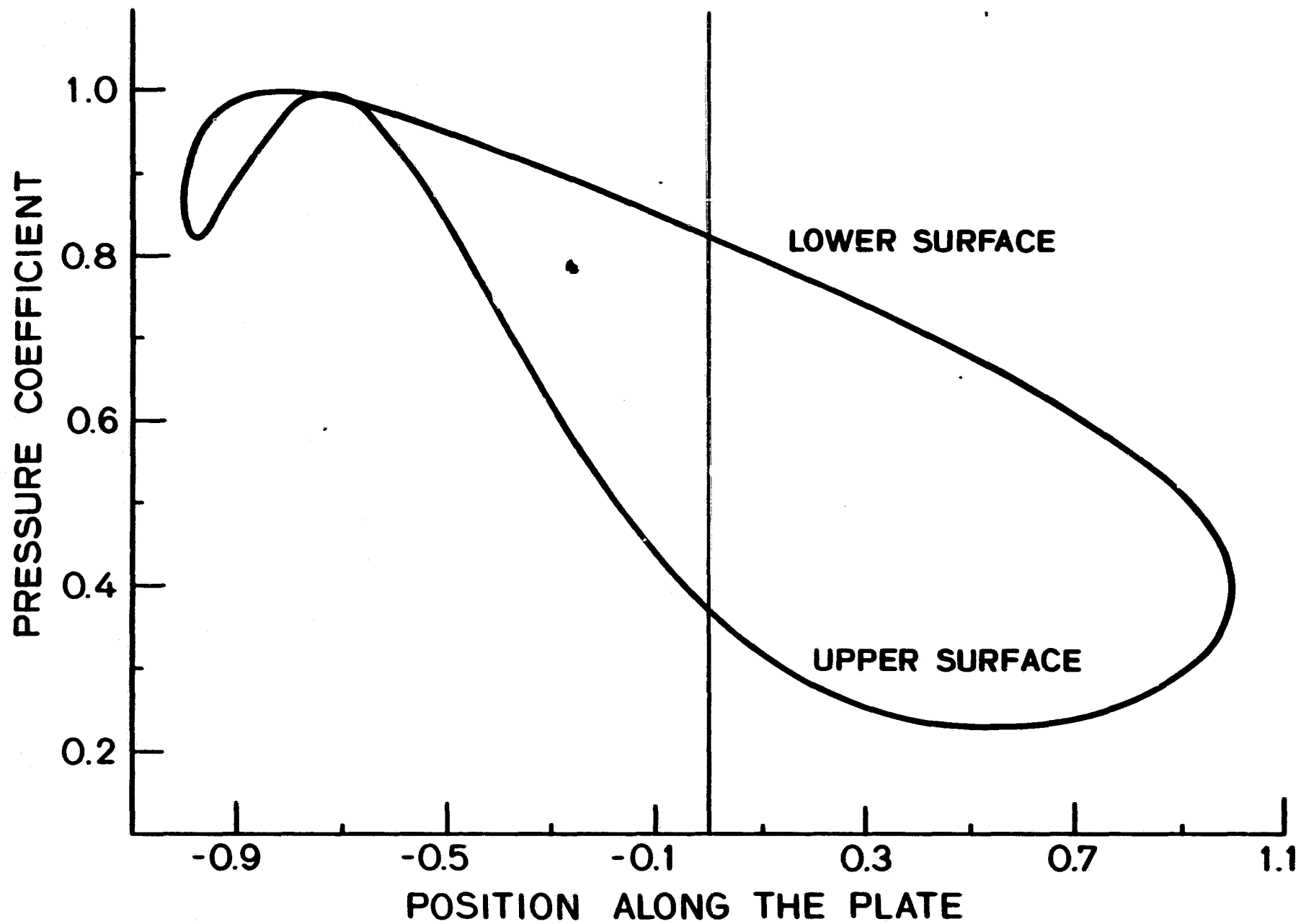


Figure 11b. Pressure distribution along the plate for $\alpha = 30$ deg.

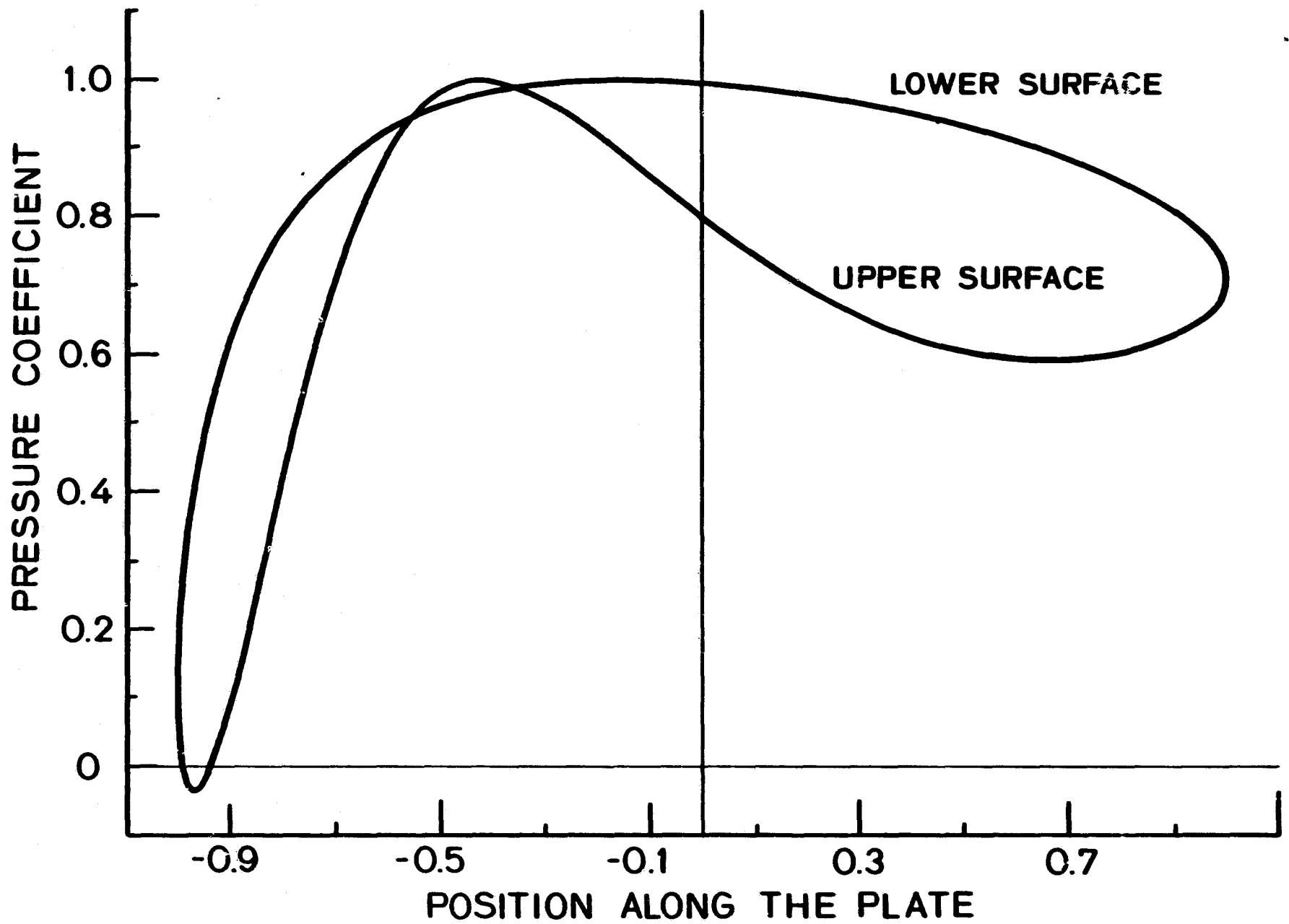


Figure 11c. Pressure distribution along the plate for $\alpha = 45$ deg.

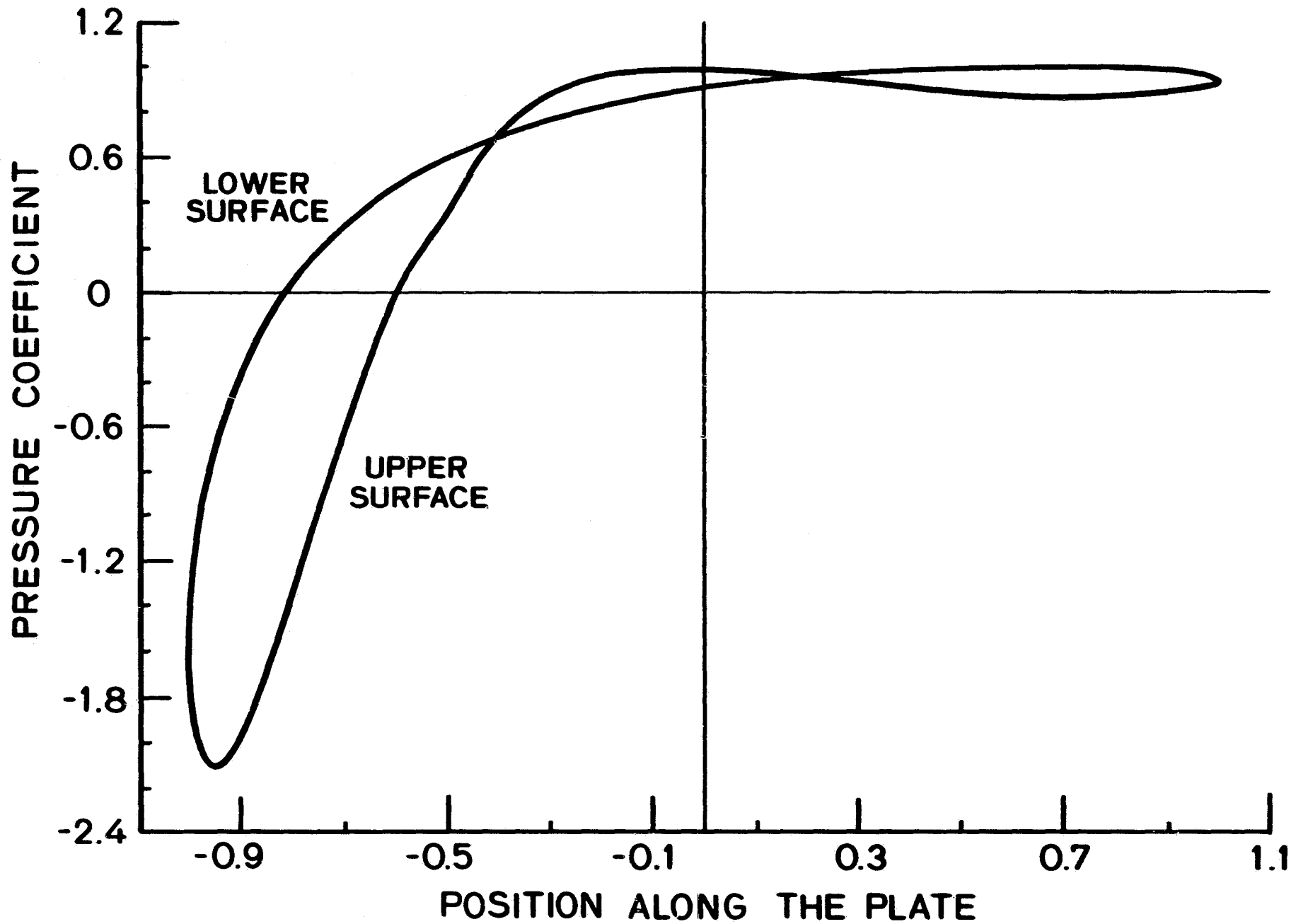
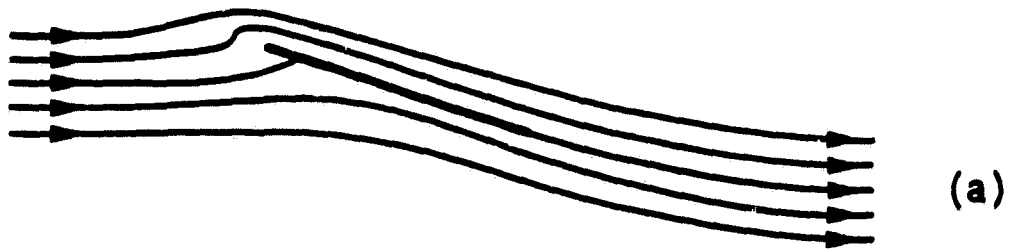
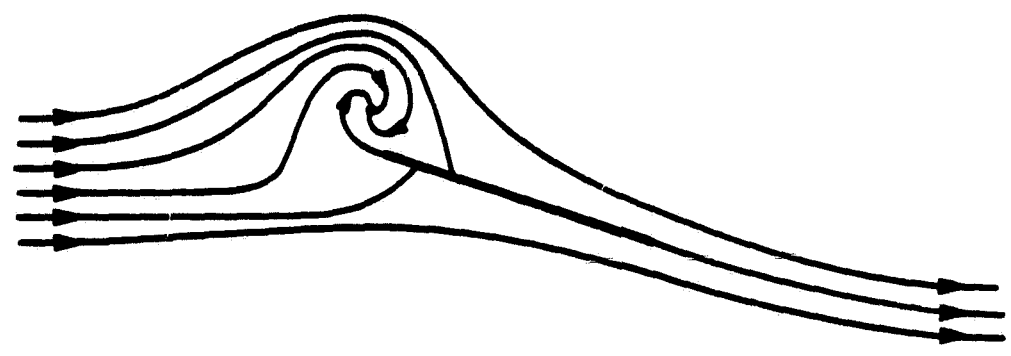


Figure 11d. Pressure distribution along the plate for $\alpha = 60$ deg.



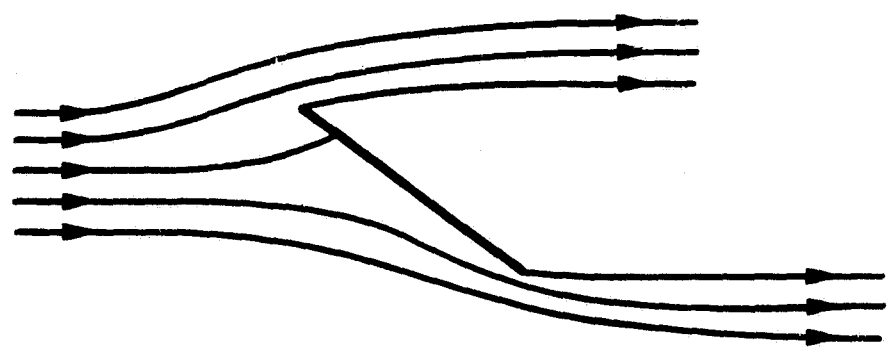
(a)

a. Totally attached flow.



(b)

b. Partially separated flow.



(c)

c. Totally separated flow.

Figure 12. Schematic of the flow over a flat plate at an angle of attack, according to three different models.

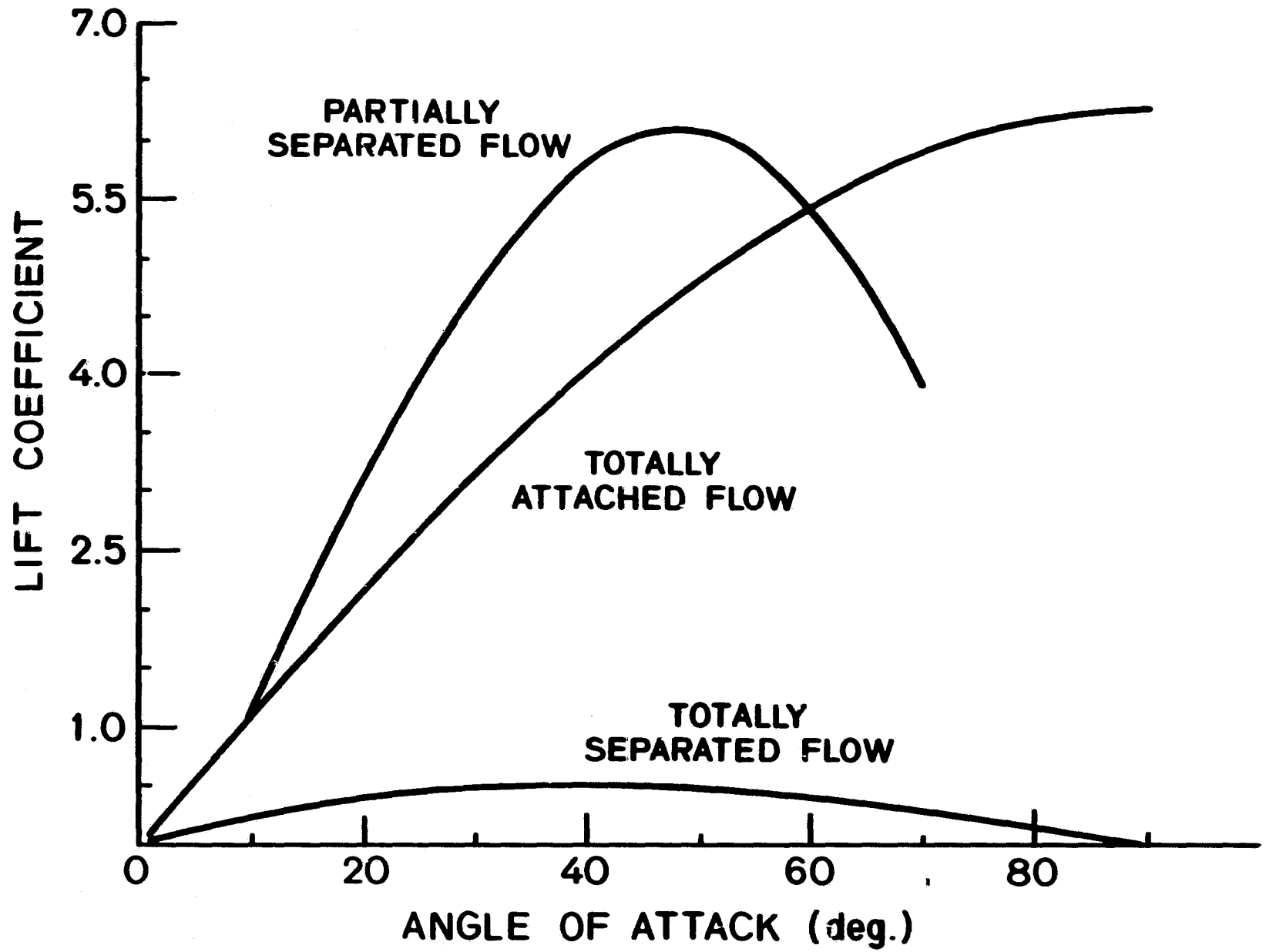


Figure 19. Lift characteristics.

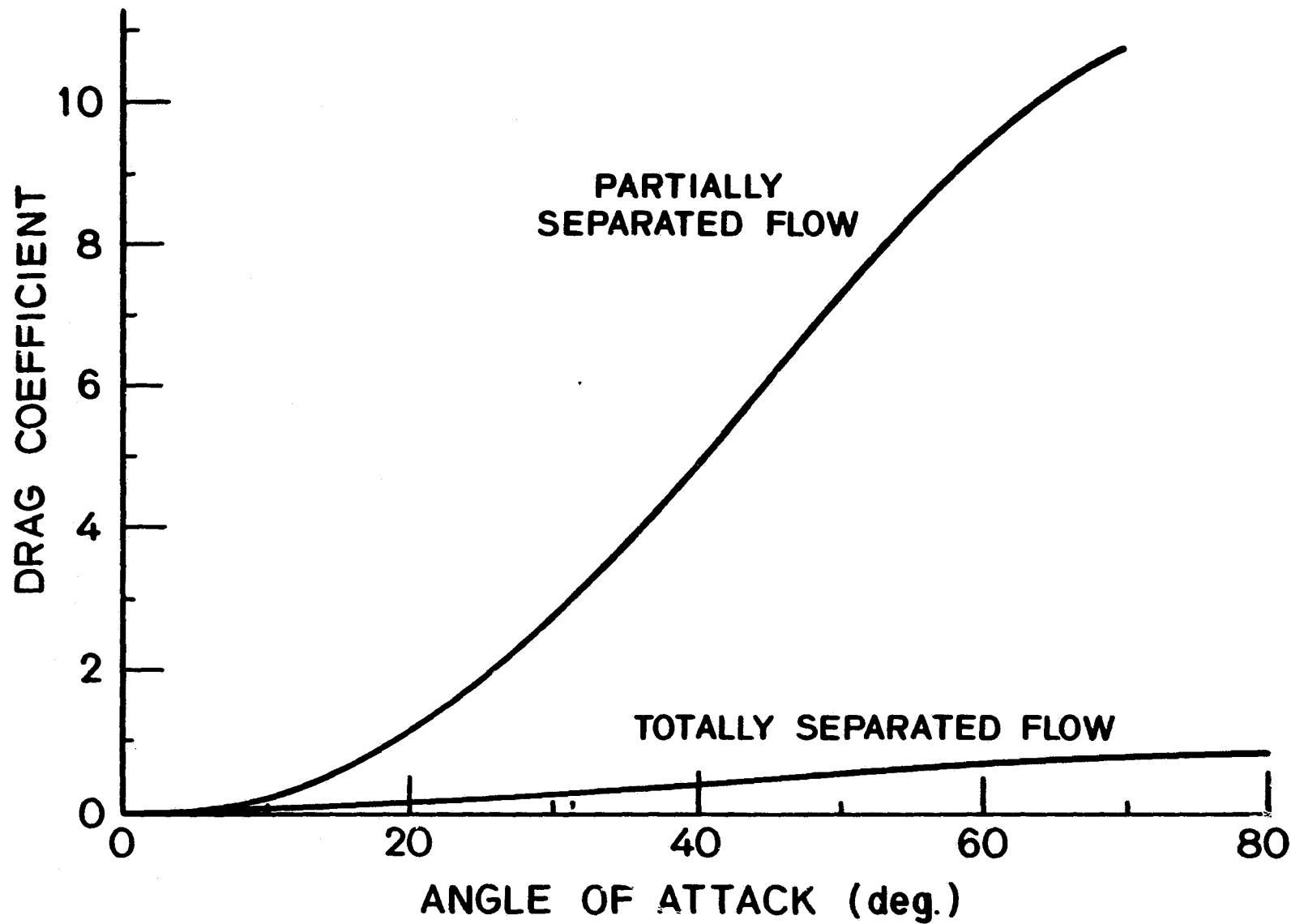


Figure 14. Drag characteristics.

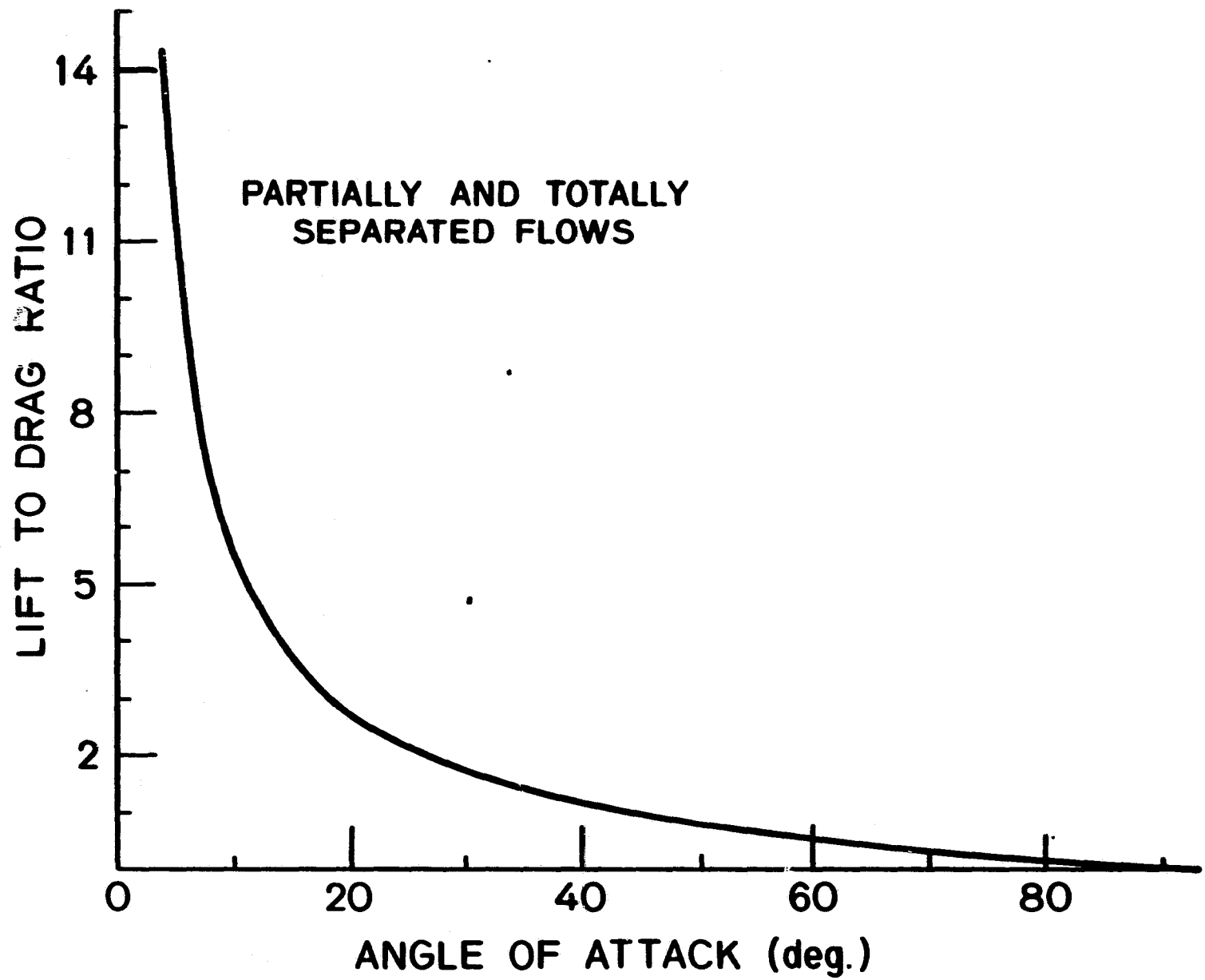


Figure 15. Lift to drag ratio versus angle of attack.

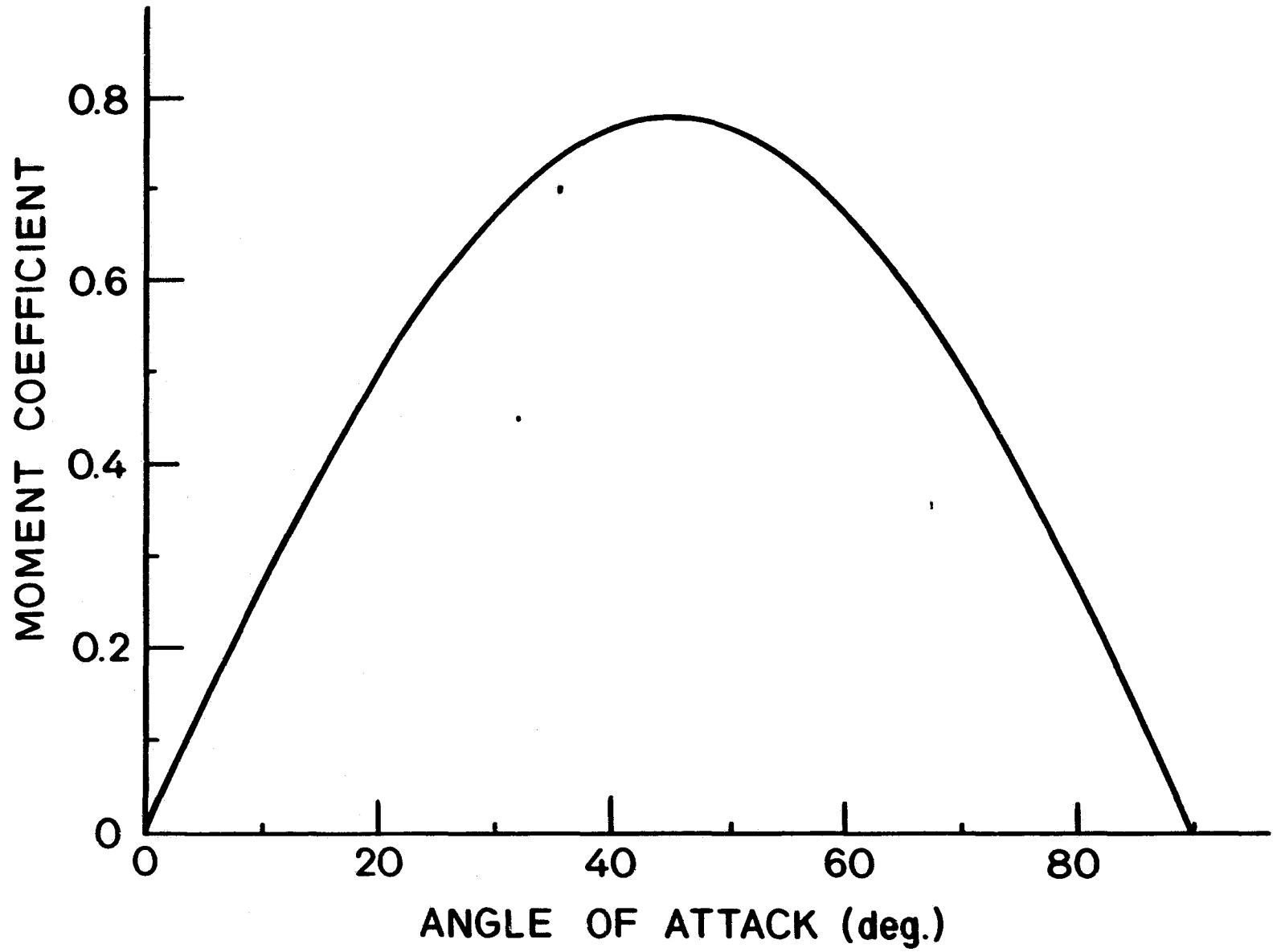


Figure 16. Pitching moment characteristic.

APPENDIX 1

A1.1

Consider a vortex of strength k_1 at the point z_1 outside of a cylinder $|z| = a$. Then, the complex potential is

$$\begin{aligned} w &= f(z) + \bar{f}\left(\frac{a^2}{z}\right) \\ &= ik_1 \ln(z - z_1) - ik_1 \ln\left(\frac{a^2}{z} - \bar{z}_1\right) \end{aligned}$$

according to the circle theorem (reference 2) w can also be written as

$$w = ik_1 \ln z + ik_1 \ln(z - z_1) - ik_1 \ln\left(z - \frac{a^2}{\bar{z}_1}\right) + \text{const.}$$

which shows three vortices: one at the point z_1 ; one at the point $\frac{a^2}{\bar{z}_1}$ which is the inverse square point of z_1 with respect to the cylinder; and one at the origin (center of the cylinder).

A1.2

Consider a sink of strength m_1 at the point z_1 outside of a cylinder $|z| = a$. Then, the complex potential is

$$\begin{aligned} w &= f(z) + \bar{f}\left(\frac{a^2}{z}\right) \\ w &= m_1 \ln(z - z_1) + m_1 \ln\left(\frac{a^2}{z} - \bar{z}_1\right) \end{aligned}$$

or

$$w = -m_1 \ln z + m_1 \ln(z - z_1) + m_1 \ln\left(z - \frac{a^2}{\bar{z}_1}\right) + \text{const.}$$

equivalent to: a sink at the point z_1 , a sink at the point $\frac{a^2}{\bar{z}_1}$, and a source at the origin.

APPENDIX 2

A four-dimensional Newton-Raphson algorithm has been used to solve the system of equations (32), (33), (34), and (35) for R_1 , θ_1 , K_0 , K_1 after elimination of M_1 from equation (49).

PROGRAM NR4D

REAL KO,K1,K,J2,J3,J4,J5,J6,J7,I1,I2,I3,I4,I5,I6,I7,I8,I9

C-----
C DATA
C-----

ALFA=?
ALF=ALFA*3.14159/180.0
30 WRITE (5,110)
110 FORMAT (' GIVE UNDERRELAXATION FACTOR')
READ (5,120) C
120 FORMAT (F)
C T=THETA, R=R1
R=?
T=?
KO=?
K1=?
10 WRITE (5,100) R,T,KO,K1
100 FORMAT (4E15.6)

C-----
T1=6*T+2*ALF
T2=2*T-2*ALF
T3=T+ALF
K=KO+K1
C-----

C-----
A1=2*R**4*(R*R-1)*(9*R*R-5)*COS(T)*COS(T1)
A2=-4*R*R*(R*R-1)*(7*R*R-3)*COS(T)*COS(4*T)
A3=2*(R*R-1)*(5*R*R-1)*COS(T)*COS(T2)
A4=-2*R**4*(9*R**4-5)*SIN(T)*SIN(T1)
A5=4*R*R*(7*R**4-3)*SIN(T)*SIN(4*T)-2*(5*R**4-1)*SIN(T)*SIN(T2)
A6=-4*KO*R**5*(4*R*R-3)*SIN(T1)+8*KO*R**3*(3*R*R-2)*SIN(4*T)
A7=-4*KO*R*(2*R*R-1)*SIN(T2)+12*K1*R**5*SIN(T1)
A8=2*K1*R**3*(21*R*R-22)*SIN(4*T)+14*K1*R**3*(3*R*R-2)*COS(4*T)
A9=8*K1*R*(3*R*R-1)*SIN(T2)+12*K1*R*(2*R*R-1)*COS(T2)
B1=6*R*(K1+K*TAN(ALF))*(COS(4*ALF)-SIN(4*ALF))
B2=-12*R**5*K*TAN(ALF)*COS(T1)
B3=3*K*R**3*(14*R*R-4)*TAN(ALF)*COS(4*T)
B4=14*K*R**3*(3*R*R-2)*TAN(ALF)*SIN(T)
B5=K*R*TAN(ALF)*(8*(3*R*R-2)*COS(T2)+12*(2*R*R-1)*SIN(T2))
C-----

C-----
A11 = A1+A2+A3+A4+A5+A6+A7+A8+A9+B1+B2+B3+B4+B5
C-----

C-----
B6=-2*R**5*(R*R-1)**2*(SIN(T)*COS(T1)+6*COS(T)*SIN(T1))
B7=4*R**3*(R*R-1)**2*(SIN(T)*COS(4*T)+4*COS(T)*SIN(4*T))
B8=-2*R*(R*R-1)**2*(SIN(T)*COS(T2)+2*COS(T)*SIN(T2))
B9=-2*R**5*(R**4-1)*(COS(T)*SIN(T1)+6*SIN(T)*COS(T1))
C1=4*R**3*(R**4-1)*(COS(T)*SIN(4*T)+4*SIN(T)*COS(4*T))
C2=-2*R*(R**4-1)*(COS(T)*SIN(T2)+2*SIN(T)*COS(T2))
C3=-12*KO*R**6*(R*R-1)*COS(T1)+16*KO*R**4*(R*R-1)*COS(4*T)
C4=-4*KO*R*R*(R*R-1)*COS(T2)+12*K1*R**6*COS(T1)
C5=4*K1*R**4*(7*R*R-11)*COS(4*T)-28*K1*R**4*(R*R-1)*SIN(4*T)
C6=4*K1*R*R*(3*R*R-2)*COS(T2)-12*K1*R*R*(R*R-1)*SIN(T2)
C7=4*K*R**4*TAN(ALF)*(3*R*R*SIN(T2)-(7*R*R-3)*SIN(4*T))
C8=28*K*R**4*(R**2-1)*TAN(ALF)*COS(4*T)
C9=-4*K*R*R*TAN(ALF)*((3*R*R-4)*SIN(T2)-3*(R*R-1)*COS(T2))
C-----

C-----
A12 = B6+B7+B8+B9+C1+C2+C3+C4+C5+C6+C7+C8+C9
C-----

C-----
D1=-2*R**6*(R*R-1)*SIN(T1)+4*R**4*(R*R-1)*SIN(4*T)
D2=-2*R*R*(R*R-1)*SIN(T2)
C-----

$D3=3*(R*R-1)*TAN(ALF)*(COS(4*ALF)-SIN(4*ALF))$
 $D4=-2*R**6*TAN(ALF)*COS(T1)+R**4*(7*R*R-3)*TAN(ALF)*COS(4*T)$
 $D5=7*R**4*(R*R-1)*TAN(ALF)*SIN(T)$
 $D6=2*R*R*(3*R*R-4)*TAN(ALF)*COS(T2)$
 $D7=6*R*R*(R*R-1)*TAN(ALF)*SIN(T2)$

 $A13=D1+D2+D3+D4+D5+D6+D7$

$D8=2*R**6*SIN(T1)+R**4*(7*R*R-11)*SIN(4*T)$
 $D9=7*R**4*(R*R-1)*COS(4*T)+2*R*R*(3*R*R-2)*SIN(T2)$
 $E1=6*R*R*(R*R-1)*COS(T2)$
 $E2=3*(1+TAN(ALF))*(R*R-1)*(COS(4*ALF)-SIN(4*ALF))$
 $E3=-2*R**6*TAN(ALF)*COS(T1)+R**4*(7*R*R-3)*TAN(ALF)*COS(4*T)$
 $E4=7*R**4*(R*R-1)*TAN(ALF)*SIN(T)$
 $E5=2*R*R*TAN(ALF)*((3*R*R-4)*COS(T2)+3*(R*R-1)*SIN(T2))$

 $A14=D8+D9+E1+E2+E3+E4+E5$

$E6=2*R**4*(R*R-1)*(9*R*R-5)*COS(T)*SIN(T1)$
 $E7=-4*R*R*(R*R-1)*(7*R*R-3)*COS(T)*SIN(4*T)$
 $E8=2*(R*R-1)*(5*R*R-1)*COS(T)*SIN(T2)$
 $E9=2*R**4*(9*R**4-5)*SIN(T)*COS(T1)$
 $G1=-4*R*R*(7*R**4-3)*SIN(T)*COS(4*T)+2*(5*R**4-1)*SIN(T)*COS(T2)$
 $G2=4*K0*R**5*(4*R*R-3)*COS(T1)-8*K0*R**3*(3*R*R-2)*COS(4*T)$
 $G3=4*K0*R*(2*R*R-1)*COS(T2)-12*K1*R**5*COS(T1)$
 $G4=-2*K1*R**3*((21*R*R-22)*COS(4*T)+7*(3*R*R-2)*SIN(4*T))$
 $G5=-4*K1*R*(2*(3*R*R-1)*COS(T2)+3*(2*R*R-1)*SIN(T2))$
 $G6=-6*(K1-K*TAN(ALF))*R*(COS(4*ALF)-SIN(4*ALF))$
 $G7=-12*K*R**5*TAN(ALF)*SIN(T1)$
 $G8=K*R**3*TAN(ALF)*(3*(14*R*R-4)*SIN(4*T)+14*(3*R*R-2)*COS(4*T))$
 $G9=4*K*R*TAN(ALF)*(2*(3*R*R-2)*SIN(T2)+3*(2*R*R-1)*COS(T2))$

 $A21 = E6+E7+E8+E9+G1+G2+G3+G4+G5+G6+G7+G8+G9$

$I1=2*R**5*(R*R-1)**2*(-SIN(T)*SIN(T1)+6*COS(T)*COS(T1))$
 $I2=-4*R**3*(R*R-1)**2*(-SIN(T)*SIN(4*T)+4*COS(T)*COS(4*T))$
 $I3=2*R*(R*R-1)**2*(-SIN(T)*SIN(T2)+2*COS(T)*COS(T2))$
 $I4=2*R**5*(R**4-1)*(COS(T)*COS(T1)-6*SIN(T)*SIN(T1))$
 $I5=-4*R**3*(R**4-1)*(COS(T)*COS(4*T)-4*SIN(T)*SIN(4*T))$
 $I6=2*R*(R**4-1)*(COS(T)*COS(T2)-2*SIN(T)*SIN(T2))$
 $I7=-4*K0*R*R*(R*R-1)*(3*R**4*SIN(T1)+SIN(T2)-4*R*R*SIN(4*T))$
 $I8=4*K1*R**4*(3*R*R*SIN(T1)+(7*R*R-11)*SIN(4*T))$
 $I9=-4*K1*R*R*(7*R*R*(R*R-1)*COS(4*T)-(3*R*R-2)*SIN(T2))$
 $P1=-12*K1*R*R*(R*R-1)*COS(T2)$
 $P2=-4*K*R**4*TAN(ALF)*(3*R*R*COS(T1)-(7*R*R-3)*COS(4*T))$
 $P3=-28*K*R**4*(R**2-1)*TAN(ALF)*SIN(4*T)$
 $P4=4*K*R*R*TAN(ALF)*((3*R*R-4)*COS(T2)-3*(R*R-1)*SIN(T2))$

 $A22 = I1+I2+I3+I4+I5+I6+I7+I8+I9+P1+P2+P3+P4$

$P5=2*R*R*(R*R-1)*(R**4*COS(T1)-2*R*R*COS(4*T)+COS(T2))$
 $P6=3*(R*R-1)*TAN(ALF)*(COS(4*ALF)-SIN(4*ALF))$
 $P7=-2*R**6*TAN(ALF)*SIN(T1)$
 $P8=R**4*TAN(ALF)*((7*R*R-3)*SIN(4*T)+7*(R*R-1)*COS(4*T))$
 $P9=2*R*R*TAN(ALF)*((3*R*R-4)*SIN(T2)+3*(R*R-1)*COS(T2))$

 $A23=P5+P6+P7+P8+P9$

$Q1=-R**4*(2*R*R*COS(T1)+(7*R*R-11)*COS(4*T)+7*(R*R-1)*SIN(4*T))$
 $Q2=-2*R*R*((3*R*R-2)*COS(T2)+3*(R*R-1)*SIN(T2))$

$$\begin{aligned}
Q3 &= -3 * (1 - \tan(\alpha)) * (R * R - 1) * (\cos(4 * \alpha) - \sin(4 * \alpha)) \\
Q4 &= -2 * R * 6 * \tan(\alpha) * \sin(T1) \\
Q5 &= R * 4 * \tan(\alpha) * ((7 * R * R - 3) * \sin(4 * T) + 7 * (R * R - 1) * \cos(4 * T)) \\
Q6 &= 2 * R * R * \tan(\alpha) * ((3 * R * R - 4) * \sin(T2) + 3 * (R * R - 1) * \cos(T2))
\end{aligned}$$

$$A24 = Q1 + Q2 + Q3 + Q4 + Q5 + Q6$$

$$\begin{aligned}
A31 &= 2 * (2 * \sin(\alpha) - K) * (R - \cos(T3)) + 2 * K1 * R + 2 * K * \tan(\alpha) * \sin(T3) \\
A32 &= 2 * R * (2 * \sin(\alpha) - K) * \sin(T3) + 2 * K * R * \tan(\alpha) * \cos(T3) \\
A33 &= -(1 + R * R - 2 * R * \cos(T3)) + 2 * R * \tan(\alpha) * \sin(T3) \\
A34 &= -(1 + R * R - 2 * R * \cos(T3)) + R * R - 1 + 2 * R * \tan(\alpha) * \sin(T3)
\end{aligned}$$

$$\begin{aligned}
A41 &= 2 * (2 * \sin(\alpha) + K) * (R + \cos(T3)) + 2 * K * \tan(\alpha) * \sin(T3) - 2 * K1 * R \\
A42 &= 2 * K * R * \tan(\alpha) * \cos(T3) - 2 * R * (2 * \sin(\alpha) + K) * \sin(T3) \\
A43 &= 1 + R * 2 + 2 * R * \cos(T3) + 2 * R * \tan(\alpha) * \sin(T3) \\
A44 &= 1 + R * 2 + 2 * R * \cos(T3) + 2 * R * \tan(\alpha) * \sin(T3) - (R * R - 1)
\end{aligned}$$

$$\begin{aligned}
FA &= 2 * R * (R * R - 1) * 2 * \cos(T) * (R * 4 * \cos(T1) - 2 * R * R * \cos(4 * T) + \cos(T2)) \\
FB &= -2 * R * (R * 4 - 1) * \sin(T) * (R * 4 * \sin(T1) - 2 * R * R * \sin(4 * T) + \sin(T2)) \\
FC &= -2 * K0 * R * R * (R * R - 1) * (R * 4 * \sin(T1) - 2 * R * R * \sin(4 * T) + \sin(T2)) \\
FD &= 2 * K1 * R * 6 * \sin(T1) \\
FE &= K1 * R * 4 * ((7 * R * R - 11) * \sin(4 * T) + 7 * (R * R - 1) * \cos(4 * T)) \\
FG &= 2 * K1 * R * R * ((3 * R * R - 2) * \sin(T2) + 3 * (R * R - 1) * \cos(T2)) \\
FH &= 3 * (K1 + K * \tan(\alpha)) * (R * R - 1) * (\cos(4 * \alpha) - \sin(4 * \alpha)) \\
FI &= -2 * K * R * 6 * \tan(\alpha) * \cos(T1) \\
FJ &= K * R * 4 * \tan(\alpha) * ((7 * R * R - 3) * \cos(4 * T) + 7 * (R * R - 1) * \sin(4 * T)) \\
FK &= 2 * K * R * R * \tan(\alpha) * ((3 * R * R - 4) * \cos(T2) + 3 * (R * R - 1) * \sin(T2))
\end{aligned}$$

$$F1 = FA + FB + FC + FD + FE + FG + FH + FI + FJ + FK$$

$$\begin{aligned}
FL &= 2 * R * (R * R - 1) * 2 * \cos(T) * (R * 4 * \sin(T1) - 2 * R * R * \sin(4 * T) + \sin(T2)) \\
FM &= 2 * R * (R * 4 - 1) * \sin(T) * (R * 4 * \cos(T1) - 2 * R * R * \cos(4 * T) + \cos(T2)) \\
FN &= 2 * K0 * R * R * (R * R - 1) * (R * 4 * \cos(T1) - 2 * R * R * \cos(4 * T) + \cos(T2)) \\
FO &= -2 * K1 * R * 6 * \cos(T1) \\
FP &= -K1 * R * 4 * ((7 * R * R - 11) * \cos(4 * T) + 7 * (R * R - 1) * \sin(4 * T)) \\
FQ &= -2 * K1 * R * R * ((3 * R * R - 2) * \cos(T2) + 3 * (R * R - 1) * \sin(T2)) \\
FR &= -3 * (K1 - K * \tan(\alpha)) * (R * R - 1) * (\cos(4 * \alpha) - \sin(4 * \alpha)) \\
FS &= -2 * K * R * 6 * \tan(\alpha) * \sin(T1) \\
FT &= K * R * 4 * \tan(\alpha) * ((7 * R * R - 3) * \sin(4 * T) + 7 * (R * R - 1) * \cos(4 * T)) \\
FU &= 2 * K * R * R * \tan(\alpha) * ((3 * R * R - 4) * \sin(T2) + 3 * (R * R - 1) * \cos(T2))
\end{aligned}$$

$$F2 = FL + FM + FN + FO + FP + FQ + FR + FS + FT + FU$$

$$\begin{aligned}
FV &= (2 * \sin(\alpha) - K) * (1 + R * R - 2 * R * \cos(T3)) \\
FW &= K1 * (R * 2 - 1) + 2 * K * R * \tan(\alpha) * \sin(T3) \\
F3 &= FV + FW \\
FX &= (2 * \sin(\alpha) + K) * (1 + R * R + 2 * R * \cos(T3)) \\
FY &= 2 * K * R * \tan(\alpha) * \sin(T3) - K1 * (R * R - 1) \\
F4 &= FX + FY
\end{aligned}$$

$$\begin{aligned}
S1 &= A11 * A22 * (A33 * A44 - A43 * A34) + A11 * A23 * (A32 * A44 - A42 * A34) \\
S2 &= A11 * A24 * (A32 * A43 - A42 * A33) + A12 * A21 * (A33 * A44 - A43 * A34) \\
S3 &= A12 * A23 * (A31 * A44 - A34 * A41) + A12 * A24 * (A31 * A43 - A41 * A33) \\
S4 &= A13 * A21 * (A32 * A44 - A34 * A42) + A13 * A22 * (A31 * A44 - A34 * A41) \\
S5 &= A13 * A24 * (A31 * A42 - A41 * A32) + A14 * A21 * (A32 * A43 - A33 * A42) \\
S6 &= A14 * A22 * (A31 * A43 - A33 * A41) + A14 * A23 * (A31 * A42 - A41 * A32) \\
DET &= S1 + S2 + S3 + S4 + S5 + S6
\end{aligned}$$

$$\begin{aligned}
J2 &= F1 * A22 * (A33 * A44 - A43 * A34) + F1 * A23 * (A32 * A44 - A42 * A34) \\
J3 &= F1 * A24 * (A32 * A43 - A42 * A33) + A12 * F2 * (A33 * A44 - A43 * A34)
\end{aligned}$$

$J4=A12*A23*(F3*A44-A34*F4)+A12*A24*(F3*A43-F4*A33)$
 $J5=A13*F2*(A32*A44-A34*A42)+A13*A22*(F3*A44-A34*F4)$
 $J6=A13*A24*(F3*A42-F4*A32)+A14*F2*(A32*A43-A33*A42)$
 $J7=A14*A22*(F3*A43-A33*F4)+A14*A23*(F3*A42-F4*A32)$
 $H1=(J2+J3+J4+J5+J6+J7)/DET$

C-----

$U1=A11*F2*(A33*A44-A43*A34)+A11*A23*(F3*A44-F4*A34)$
 $U2=A11*A24*(F3*A43-F4*A33)+F1*A21*(A33*A44-A43*A34)$
 $U3=F1*A23*(A31*A44-A34*A41)+F1*A24*(A31*A43-A41*A33)$
 $U4=A13*A21*(F3*A44-A34*F4)+A13*F2*(A31*A44-A34*A41)$
 $U5=A13*A24*(F4*A31-F3*A41)+A14*A21*(F3*A43-F4*A42)$
 $U6=A14*F2*(A31*A43-A33*A41)+A14*A23*(F4*A31-F3*A41)$
 $H2=(U1+U2+U3+U4+U5+U6)/DET$

C-----

$V1=A11*A22*(F3*A44-F4*A34)+A11*F2*(A32*A44-A42*A34)$
 $V2=A11*A24*(A32*F4-A42*F3)+A12*A21*(F3*A44-F4*A34)$
 $V3=A12*F2*(A31*A44-A34*A41)+A12*A24*(A31*F4-A41*F3)$
 $V4=F1*A21*(A32*A44-A34*A42)+F1*A22*(A31*A44-A34*A41)$
 $V5=F1*A24*(A31*A42-A41*A32)+A14*A21*(A32*F4-F3*A42)$
 $V6=A14*A22*(A31*F4-F3*A41)+A14*F2*(A31*A42-A41*A32)$
 $H3=(V1+V2+V3+V4+V5+V6)/DET$

C-----

$W1=A11*A22*(A33*F4-A43*F3)+A11*A23*(A32*F4-A42*F3)$
 $W2=A1*F2*(A32*A43-A42*A33)+A12*A21*(A33*F4-A43*F3)$
 $W3=A12*A23*(A31*F4-A41*F3)+A12*F2*(A31*A43-A41*A33)$
 $W4=A13*A21*(A32*F4-A42*F3)+A13*A22*(A31*F4-A41*F3)$
 $W5=A13*F2*(A31*A42-A41*A32)+F1*A21*(A32*A43-A33*A42)$
 $W6=F1*A22*(A31*A43-A33*A41)+F1*A23*(A31*A42-A41*A32)$
 $H4=(W1+W2+W3+W4+W5+W6)/DET$

C-----

$R=R-C*H1$
 $T=T-C*H2$
 $KO=KO-C*H3$
 $K1=K1-C*H4$
 IF (ABS(H1).LT.1.E-3.AND.ABS(H2).LT.1.E-3) GO TO 20
 IF (ABS(H3).LT.1.E-3.AND.ABS(H4).LT.1.E-3) GO TO 20
 GO TO 10
 20 WRITE (5,100) R,T,KO,K1
 WRITE (5,130)
 130 FORMAT (' IF YOU WANT ANOTHER RELAXATION FACTOR, TYPE 1')
 READ (5,140) IFF
 140 FORMAT (I)
 IF (IFF.EQ.1) GO TO 30
 STOP
 END